Review

Metallogenic Model and Prospecting Progress of the Qiandongshan–Dongtangzi Large Pb-Zn Deposit, Fengtai Orefield, West Qinling Orogeny

Ruiting Wang [1,*], Zhenjia Pang [1], Qingfeng Li [1], Geli Zhang [2], Jiafeng Zhang [2], Huan Cheng [1], Wentang Wu [3] and Hongbo Yang [3]

1   Northwest Nonferrous Geological and Mining Group Co., Ltd., Xi'an 710054, China
2   Baoji No. 717 Corps Limited of Northwest Nonferrous Geological and Mining Group, Baoji 721015, China
3   Shananxi Northwest Nonferrous Lead and Zinc Group Co., Ltd., Baoji 721015, China
*   Correspondence: wrtyf@163.com; Tel.: +86-13659288199

Abstract: The Qiandongshan–Dongtangzi large Pb-Zn deposit is located in the Fengxian–Taibai (abbr. Fengtai) polymetallic orefield. The ore bodies primarily occur within and around the contact surface between the limestone of the Gudaoling Formation and the phyllite of the Xinghongpu Formation, which are clearly controlled by anticline and specific lithohorizon. Magmatic rocks are well developed in the mining area, consisting mainly of granitoid plutons and mafic–felsic dikes. Previous metallogenic geochronology studies have yielded a narrow range of ages between 226 and 211 Ma, overlapped by the extensive magmatism during the Late Triassic period in this region. The $\omega(Co)/\omega(Ni)$ ratio of pyrite in lead–zinc ore ranges from 4.44 to 15.57 (avg. 8.56), implying that its genesis is probably related to volcanic and magmatic-hydrothermal fluids. The δD and $\delta^{18}O$ values (ranging from $-94.2‰$ to $-82‰$, and $18.89‰$ to $20.72‰$, respectively,) of the ore-bearing quartz indicate that the fluids were perhaps derived from a magmatic source. The $\delta^{34}S$ values of ore-related sulfides display a relatively narrow range of 4.29‰ to 9.63‰ and less than 10‰, resembling those of magmatic-hydrothermal origin Pb-Zn deposits. The Pb isotopic composition of the sulfides from the Qiandongshan–Dongtangzi Pb-Zn deposit (with $^{206}Pb/^{204}Pb$ ratios of 18.06 to 18.14, the $^{207}Pb/^{204}Pb$ ratios of 15.61 to 15.71, and $^{208}Pb/^{204}Pb$ ratios of 38.15 to 38.50) is similar to that of the Late Triassic Xiba granite pluton, suggesting that they share the same Pb source. The contents of W, Mo, As, Sb, Hg, Bi, Cd, and other elements associated with magmatic-hydrothermal fluids are high in lead–zinc ores, and the contents of Sn, W, Co, and Ni are also enriched in sphalerite. The contents of trace elements and rare earth elements in the ore are similar to those in the Xiba granite pluton, and they maybe propose a magmatic-hydrothermal origin as well. As a result of this information, the Qiandongshan–Dongtangzi large Pb-Zn deposit may be classified as a magmatic hydrothermal stratabound type, with the Si/Ca contact area being the ore-forming structural plane. Thus, a mineralization model has been proposed based on a comparative analysis of the geological and geochemical properties of the lead–zinc deposit in the Fengtai orefield. It is considered that the secondary anticlines developed on both wings of the Qiandongshan–Dongtangzi composite anticline are the favorable sites for Pb-Zn deposition. Accordingly, the Si/Ca plane and secondary anticline are the major ore-controlling factors and prospecting targets. The verification project was first set up on the north wing of the composite anticline, and thick lead–zinc ore bodies were found in all verification boreholes, accumulating successful experience for deep exploration of lead–zinc deposits in this region.

Keywords: metallogenic model; prospecting progress; lead–zinc deposit; Qiandongshan–Dongtangzi; Fengtai orefield

1. Introduction

The Fengxian–Taibai (abbr. Fengtai) orefield in the Shaanxi Province, which belongs to the middle of the Qinling polymetallic metallogenic belt, is located in the northern margin of the South Qinling orogenic belt, and adjacent to the Shangdan suture zone. It is a famous place for the origin of mineral resources of lead, zinc, gold, etc. [1–3] The lead–zinc deposits were formed in the Late Triassic period and are mainly stratified and stratiform-like in the saddle and the two wings of the anticlinal fold. Since the beginning of this century, with the continuous discovery of shallow surface minerals in this region, the geological prospecting work in the orefield has shifted t the blind stage of depth exploration. Significant progress has been made over the past few decades in the exploration and metallogeny of the Fengtai orefield, represented by the Qiandongshan–Dongtangzi lead–zinc deposit. Exploration has been carried out in the region around the deep and peripheral parts of the known deposits, increasing the lead and zinc resources by approximately 2 million tons [4]. Research efforts on lead–zinc deposits have also deepened, with new understanding and achievements in deposit geology, geochemistry, geochronology, ore genesis, ore-controlling factors, and prospecting prediction. In particular, macro-prospecting and micro-metallogenic research have facilitated each other, which has led to a continuous improvement of the ore genesis and metallogenic model in the Fengtai orefield, showing great prospecting potential [4–8]. Based on this, combined with the prospecting experience, this paper makes a comprehensive study on the regional geological setting, geochemical characteristics, ore-controlling factors, ore-controlling rules, prospecting signs, ore genesis, and prospecting progress of the Qiandongshan–Dongtangzi lead–zinc deposit. A metallogenic model and prospecting targets were established, and exploration prediction and engineering verification were carried out, resulting in significant exploration breakthroughs.

2. Regional Geological Setting

The Fengtai orefield is known as the most developed lead–zinc deposit among the six orefields in the South Qinling metallogenic belt [3]. It is bounded in the north by the Xiangzihe fault ($F_2{}^1$), which is a part of the Lixian–Shanyang–Fengzhen fault, in the south by the Jiudianliang fault ($F_2{}^2$), which is a part of the west section of the Zhenan–Banyanzhen fault, and in the east by the Cretaceous rifted basin. The Fengtai orefield, as a part of the West Qinling orogeny, has experienced multiple tectono-magmatic activities, especially during the Indosinian period. Correspondingly, various structures are extremely developed, forming approximately rhomboid tectonic units composed of WNW-trending folds and WNW-trending faults (Figure 1).

The outcropping strata in the region are mainly the Middle Devonian Gudaoling Formation, the Late Devonian Xinghongpu Formation, and the Jiuliping Formation (Figure 1). The characteristics of each strata are shown in Figure 2.

The Gudaoling Formation occupies the core of regional WNW-trending anticline, and the Xinghongpu Formation is distributed on the two wings of the WNW-trending anticline. The Jiuliping Formation constitutes the core of regional WNW-trending Guchahe–Yinjiaba syncline (I level). In addition, the Triassic flysch Formation is exposed to the south of the compound fold, while the Cretaceous sedimentary is developed in the north. The WNW-trending faults are well developed in the Fengtai orefield, and the NE-trending faults are mostly post-mineralization faults with some degree of dislocations to the ore bodies.

The intermediate felsic dikes are well developed in the Fengtai orefield. The major intrusions are the Xiba and the Huahongshuping granitic plutons, which are distributed in the central part of the Fengtai orefield and are basically consistent with the direction of the main structural line (NW direction) within the area [6,9] (Zhang, 2010; Hu, 2015). The largest Xiba pluton is mainly composed of granodiorite, quartz diorite, and monzogranite, with hornstone and andalusite developed in the outer contact zone. A combination of previous zircon U-Pb ages indicate that the granitic complex intruded between 219 and 215 Ma [9–11]. The previous geochronoloical and geochemical data suggested that the Xiba pluton was formed in the Late Indosinian period, and was emplaced under the post-

collision setting after the collision between the North China Craton and the Yangtze Craton along the Mianlue suture zone [1,12,13] The Shuangwang large gold deposit is developed approximately 5 km north of the Xiba pluton, and the Yinmusi medium-sized lead–zinc deposit is developed approximately 15 km in the NW direction. It is believed that the Xiba pluton may provide heat energy and ore-forming material for mineralization [2,14–16]. The Huahongshuping pluton, which was emplaced in the Devonian strata, consists mainly of medium-fine granodiorite, with Late Triassic zircon U-Pb age (214.3 ± 2.7 Ma [8]. Hornfels, skarnization, and wolframite mineralization were locally formed in the contact zone between the Huahongshuping pluton and the wall-rock. Large quantities of marble have been found in the Changgou, Donggou, and other lead–zinc deposits to the south of the Huahongshuping pluton. Barite veins have been locally filled along faults, all of which should be genetically related to the Huahongshuping pluton. Moreover, many kinds of dikes are widely developed individually or in groups, filling in the WNW- and NE-trending faults, ranging from tens of centimeters to several meters in width and tens of meters to 3–4 km in length. Among them, the WNW-trending dikes are dominated by granite porphyry, and the NE-trending dikes are mainly diorite porphyrite and lamprophyre. In addition, there are the Hejiazhuang pluton and Taibai pluton to the northwest and northeast of the orefield.
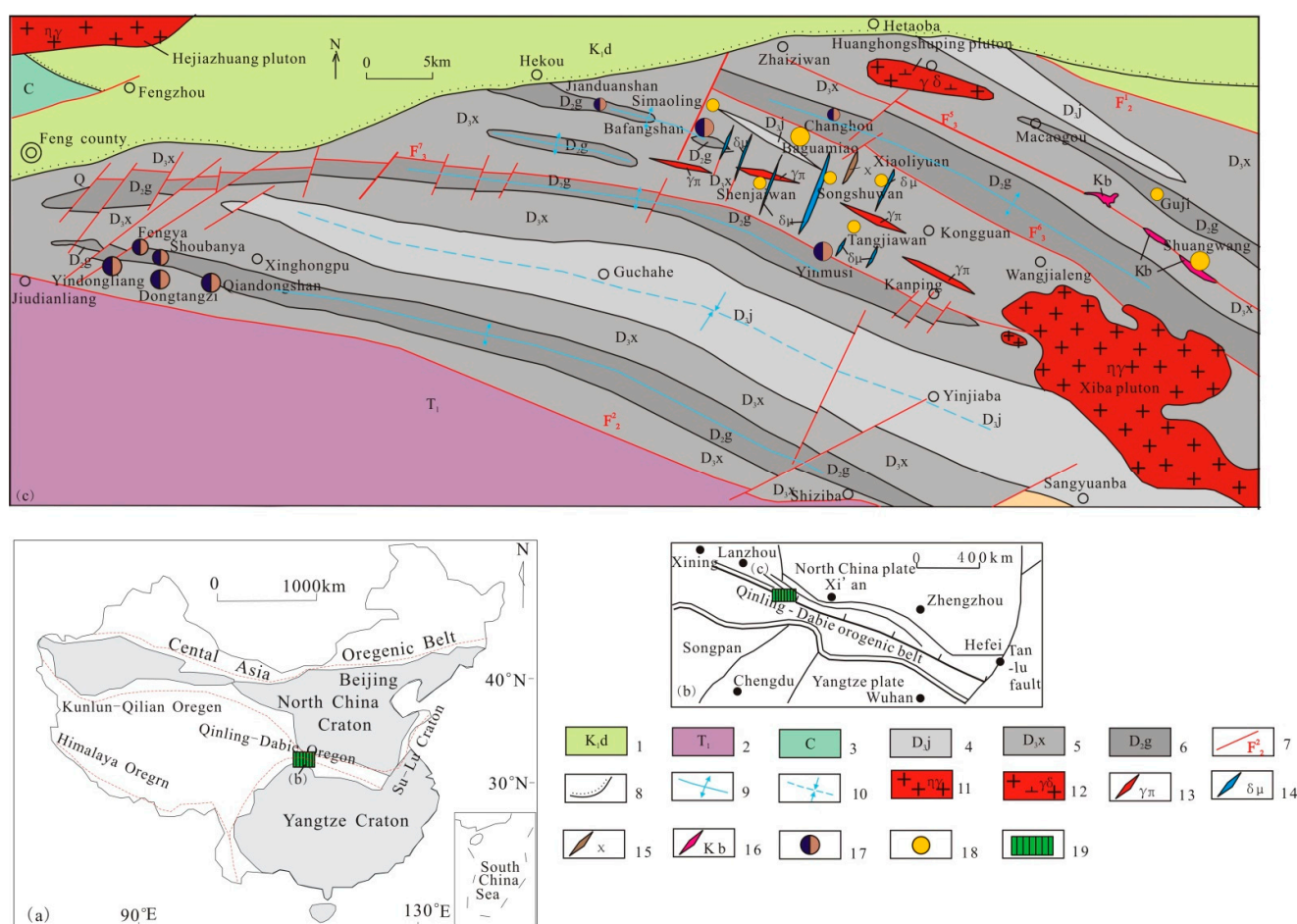

Figure 1. (**a**)—The location map of the study area in China; (**b**)—The location of the study area in the Qinling metallogenic bel; (**c**)—Geological Sketch Map of Mineral Deposits in Fengtai Polymetallic Orefield; 1—Cretaceous Donghe group; 2—Lower Triassic; 3—Carboniferous; 4—Upper Devonian Jiuliping formation; 5—Upper Devonian Xinghongpu Formation; 6—Middle Devonian Gudaoling Formation; 7—Faults and number; 8—Angular unconformity; 9—Axis of synclinorium; 10—Axis of anticline; 11—Monzogranite; 12—Granodiorite; 13—Granite-porphyry dike; 14—Diorite porphyrite dike; 15—Lamprophyre dike; 16—Albite breccia; 17—Lead–zinc deposit (the size is proportional to ore body mass); 18—Gold deposit (the size is proportional to ore body mass.); 19—Study region.

Formation	Code	Columnar section	Thickness	Description
Jiuliping	D_3j		1500~2500 (meter)	Metamorphic quartz sandstone and silty slate.
Xinghongpu	D_3x^3		210~660 (meter)	Iron dolomitic silty phyllite, spotted iron dolomitic silty phyllite mixed with banded marlitized limestone, and the top is carbonaceous silty phyllite. There are gold deposits present.
	D_3x^2		120-170 (meter)	Chlorite-bearing sericite phyllite with thin layers of microcrystalline limestone and ferruginous sericite phyllite. Irregular quartz veins are widely developed, and a few brachiopod fossils are contained in the thin layers of microcrystalline limestone.
	$D_3x_1^2$		300 (meter)	Ferridolomitic sericite phyllite, locally sand wiched with a small amount of calcareous sericite phyllite.
	$D_3x_1^1$		90~180 (meter)	Carbonaceous calcareous sericite phyllite with lenti-cular, banded and thin-layer carbonaceous fine-grained limestone or thin-layer biological fine-grained limestone, followed by calcareous sericeousphyllite. Local occurr-ences of coral, brachiopods, and a few crinoid stems fossils can be observed.
Gudaoling	D_2g		>500 (meter)	Thin to middle thick layered carbonaceous biomicry-stalline limestone, bioclastic limestone, crystalline limestone, and the biological fossils. At the top, there is a layer of silicified altered rock layers with a thickness of several meters to tens of meters, which means that the top is the main ore-bearing layer for lead-zinc deposits in the area. Currently, the large and medium-sized lead-zinc deposits that have been proven are alllocated in this layer.

Figure 2. Bar Chart of Main Outcrop Strata in Fengtai Area (Main Bearing Strata of Lead, Zinc, and Gold).

The lead–zinc deposits in the Fengtai orefield are closely associated with anticline structure in this area. The lead–zinc ore bodies in the Fengtai orefield are primarily hosted in the carbon-bearing portion of the transition layer between the top of the Gudaoling Formation and the bottom of the Xinghongpu Formation, where the saddle and wings of the secondary anticline develop, as well as the WNW-trending fault. At present, the phenomenon of correlation between lead and zinc ore bodies and syncline has not been seen in the orefield. From north to south, there are six sub-anticlines (II level), corresponding to six lead–zinc ore belts: (1) the Changgou–Donggou lead–zinc ore belt, with the Baiyanggou, Changgou, Yindongshan, Liushugou, Donggou, Yafangwan, and other small lead–zinc deposits. (2) the Jianduanshan–Bafangshan–Erlihe lead–zinc polymetallic ore belt, with the Bafangshan–Erlihe super-large lead–zinc deposit and Jianduanshan small lead–zinc deposit. (3) the Sanjiaoya–Gangou lead–zinc ore belt, with the Gangou copper ore occurrence. (4) the Yinmusi–Daheigou lead–zinc ore belt, with the Yinmusi medium-sized lead–zinc deposit and Daheigou small-sized lead–zinc deposit. (5) the Magou–Tieluwan lead–zinc ore belt, with the lead–zinc ore occurrence in the contact zone between limestone and phyllite in Xinghongpu Formation. (6) the Qiandongshan–Shuibaigou lead–zinc ore belt is the largest metallogenic belt with the largest amount of proved resources in the area, with large-scale lead–zinc deposits such as Qiandongshan, Dongtangzi, and Yindongliang, as well as medium-sized deposits such as Fengya, Shoubanya, and Heiya.

3. Geology of Qiandongshan–Dongtangzi Lead–Zinc Deposit

3.1. Deposit Geology

3.1.1. Stratigraphy

The carbonate rocks of the Middle Devonian Gudaoling Formation (D_2g) and low-grade regionally metamorphosed argillaceous clastic rocks of the Upper Devonian Xinghongpu Formation (D_3x) are the dominant lithostratigraphic units in the mining area (Figure 3).
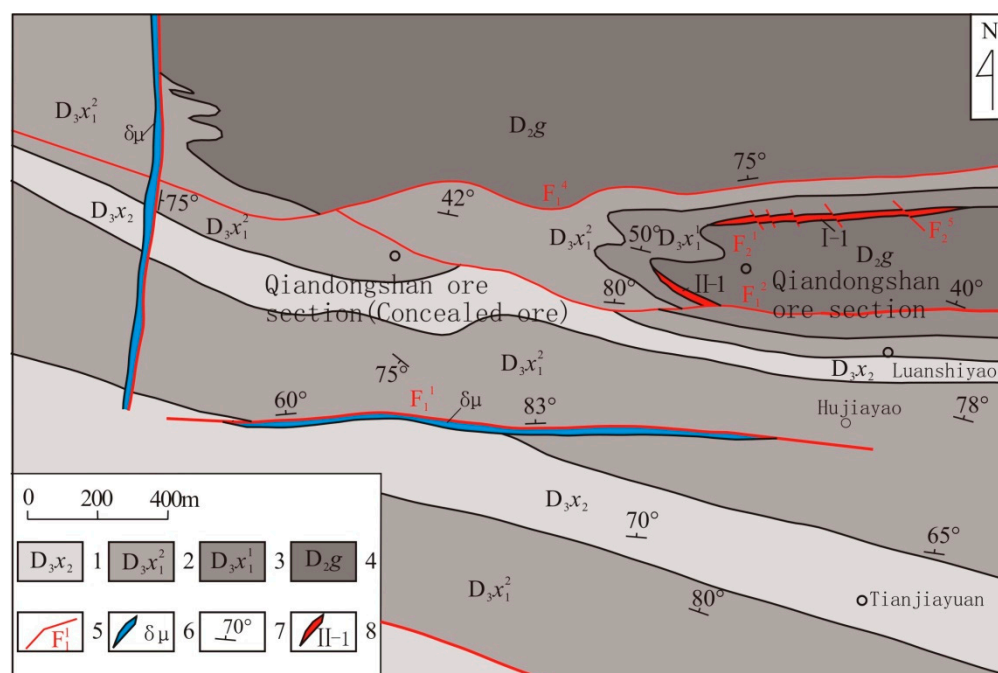
Figure 3. Geological Sketch Map of the Qiandongshan–Dongtangzi Pb-Zn Deposit; 1—The second lithologic member of the Xinghongpu Formation; 2—The second layer of the first lithologic member of the Xinghongpu formation; 3—The first layer of the first lithologic member of the Xinghongpu Formation; 4—Gudaoling Formation; 5—Faults and number; 6—Diorite porphyrite dike; 7—Attitude of stratum; 8—Lead–zinc deposit and number.

The Middle Devonian Gudaoling Formation is the core unit of the anticlinal structure of the mining area, which is mostly distributed in the central and eastern parts of the mining area. The major lithology includes thin (generally 0.01 m to 0.1 m thick) to middle thick (generally 0.1 m to 0.5 m thick) layered carbonaceous bio-microcrystalline limestone, bio-clastic limestone, crystalline limestone, and fossils of coral, stromatoporoids, and a few brachiopods. The presence of advantageous rock formations such as biolimestone and the associated structural combinations between them often occur in the same mineral deposit, making them beneficial ore-forming structural surface combinations. This is the primary reason for the top layer becoming the main ore-bearing layer of lead–zinc deposition in the mining area. The ore-hosted rocks are silicified limestone, generally several meters to tens of meters thick, which is in integrated contact with the overlying Xinghongpu Formation.

The Upper Devonian Xinghongpu Formation is widely distributed in the mining area, consisting of a set of fine clastic rocks interbedded with carbonate rocks, forming the wings of the anticlinal structure. According to the lithological combination characteristics, it can be divided into three lithological sections (Figure 2), and only the first and second lithologic sections are exposed in the mining area. The first lithological section (D_3x^1) is distributed nearly in an EW direction. The lower part ($D_3x_1^1$) mainly composed of carbonaceous calcareous sericite phyllite with lenticular, banded. and thin-layer carbonaceous fine-grained limestone or thin-layer biological fine-grained limestone, followed by calcareous sericeous phyllite. Local occurrences of coral, brachiopods, and a few crinoid stems fossils can be observed; The upper part ($D_3x_1^2$) mainly consists of ferridolomitic sericite phyllite, locally sandwiched with a small amount of calcareous sericite phyllite. The second lithological section (D_3x^2) is mainly distributed in the southern part of the mining area. It is composed of chlorite-bearing sericite phyllite with thin layers of microcrystalline limestone and ferruginous sericite phyllite. Irregular quartz veins are widely developed, and a few brachiopod fossils are contained in the thin layers of microcrystalline limestone. It has integrated contact with the overlying formation.

3.1.2. Structure Geology

(1) Fold structure

The fold structures in the mining area are mainly composed of a compound anticline consisting of Qiandongshan–Dongtangzi (III level). The secondary anticline structures (IV level) are well developed and often exhibit tight closures and overturned folds, i.e., overturned southern limb and normal northern limb.

The Qiandongshan–Dongtangzi complex anticline (III level) is located on the southwestern end of the Qiandongshan–Shangtianba–Shuibaigou complex anticline (II level), near the EW direction. The Qiandongshan–Dongtangzi complex anticline (III level) core is only exposed on the surface of Qiandongshan, with an exposed length of more than 11 km in the east–west direction and a width of approximately 120–460 m in the north–south direction. The Qiandongshan–Dongtangzi complex anticline (III level) slopes westward to the Dongtangzi and is a concealed anticline. The strike of the axial plane is oriented between 275° and 285°, with the upper portion approaching a vertical orientation and the lower portion steeply dipping towards the north. The northern wing is normal, with a dip direction angle of 354°–7° and a dip angle of 55°–79°; the southern wing is nearly vertical, with a dip direction angle of 195°–220° and a dip angle of 72°–88°. The lower part is overturned and inclined to the north, with a dip angle of 75°.

In the anticlinal hinge zone, a complex "M"-shaped double-folded structure is formed by the subordinated primary anticline structures (IV level) in the south and north, which is known as the Qiandongshan–Dongtangzi structure (III level). The northern subordinate anticline (IV level) develops on the north side of the transition end of the Qiandongshan–Dongtangzi complex anticline (III level). The strike of the northern subordinate anticlinal ridge is 288°, and the dip angle ranges from 19° to 44°. The southern subordinate anticline (IV level) is developed in the southern side of the transition end of the Qiandongshan–Dongtangzi compound anticline (III level). The southern subordinate anticline dips to the west, with a strike of 282°, and a dip angle ranging from 10° to 38°.

(2) Fault structure

The fault structure in the mining area is well developed and can be divided into two groups based on their distribution orientation: longitudinal fault and transverse fault.

① Longitudinal fault

The longitudinal faults spread in a WNW direction, and most of them developed between the interface of the Gudaoling Formation and the Xinghongpu Formation on both sides of the anticline structure, demonstrating a reverse faulting nature. These structures mainly refer to interlayer detachment faults formed prior to mineralization, which also underwent activity after mineralization, often disrupting the integrity of anticline and syncline structures. The occurrence of faults is consistent with that of the fold axial plane, and locally cut across the bedding planes. Two major longitudinal faults are the $F_1{}^2$ and $F_1{}^4$. Among them, the $F_1{}^2$ fault is a compression torsional fault, developed in the southwestern part of the mining area, and the southern limb of the Qiandongshan–Dongtangzi compound anticline. The fault has a length of over 1000 m in the surface, dipping direction from 275° to 295°, with a dip direction of north–northeast and a dip angle ranging from 61° to 88°. The fault exhibits a wavy and curved pattern, with a fracture zone width ranging from 0.05 to 3 m. This fault causes the lower part of the first lithological section of the Xinghongpu Formation ($D_3x_1{}^1$) into direct contact with the second lithological section (D_3x^2), resulting in a vertical drop of approximately 270 m and a horizontal displacement of 14 m in the footwall of the No. II ore body in the Qiandongshan area.

② Transverse fault

The transverse faults occur near the No. I-1 ore body, mainly in the NW direction and secondarily in the NE direction. They are relatively small in size but numerous, appearing at approximately equal intervals along the trend of the ore body, with spacing ranging from several tens of meters to approximately 100 m. These faults formed after the ore-forming period and often cut across the northern limb of the northern subordinate anticline, causing displacement of the strata and the ore body, and are part of the ore-breaking structure. They

mostly exhibit sub-horizontal displacement, accompanied by a small amount of vertical displacement, with horizontal displacement generally ranging from a few meters to over ten meters. This group of faults belongs to a set of the X-conjugated faults caused by shear stress.

3.1.3. Magmatic Phenomena and Hydrothermal Activity

There is no large-scale outcrop of magmatic rocks in the mining area, with only an EW-trending Indosinian diorite dike developed on the surface of the Songjiashan, intruded into the Upper Devonian Xinghongpu Formation, with approximately 1500 m in length and 1–4 m in width. The deep exploration project also revealed the presence of diorite dikes and granite porphyry dikes. The diorite dikes are spread in a NE direction, while the granite porphyry dikes exhibit an almost EW direction. The dikes mostly developed in the southern limb of the Qiandongshan–Dongtangzi compound anticline, and these dikes are intersecting with the No. II-1 ore body.

The quartz veins are very developed in the Dongtangzi lead–zinc deposit, mainly occurring along the stratiform layers. Laterally striking quartz veins are superimposed on them, and large-scale calcite–quartz veins produced in the stratiform layer are developed in the late stage. The entire mineralization process is accompanied by intense hydrothermal activity (Figure 4). Therefore, the mineralization processes of the deposit can be divided into four stages [17]: the sulphide—iron carbonate—quartz vein stage, and the massive sulfide-carbonate stage, and the low-sulfide quartz–calcite vein stage, and thick quartz–carbonate vein stage. The deep drilling control of the Dongtangzi ore section reveals a locally inclined and thick granite porphyry dike exceeding 60 m (true thickness of 30–40 m). The widespread occurrence of dikes suggests the possible existence of concealed intrusive bodies in the deep part.

Figure 4. Network quartz–sulfide veins in the Qiandongshan–Dongtangzi Pb-Zn deposit.

3.2. Geological Characteristics of Ore Body

The large lead–zinc deposit of Qiandongshan–Dongtangzi can be divided into two sections: the Qiandongshan ore section and the Dongtangzi ore section. A total of five lead–zinc bodies have been delineated in the large lead–zinc deposit of Qiandongshan–Dongtangzi, of which No. I-1 and No. II-1 ore bodies are the main ore bodies (Figure 5). The two main ore bodies currently have an estimated resource of approximately 2 million tons of lead and zinc. The ore bodies mainly occur near the Si/Ca interface in the contact zone of the biocrystalline limestone of Gudaoling Formation and the carbonaceous calcareous phyllite of Xinghongpu Formation. The ore body is strictly controlled by the "M"-shaped secondary anticline, resulting in the formation of thick ore bodies in the silicocalcium layer, that is, the size, shape, and occurrence of the ore body are controlled by the Si/Ca structural

plane. The ore body dips to the west of the fold, with its outcrop exhibiting a horizontally positioned "eight" shape at the surface of the Qiandongshan ore section. It becomes a concealed ore body dipping to the eastern side of the Dongtangzi ore section, following the structure of the fold.
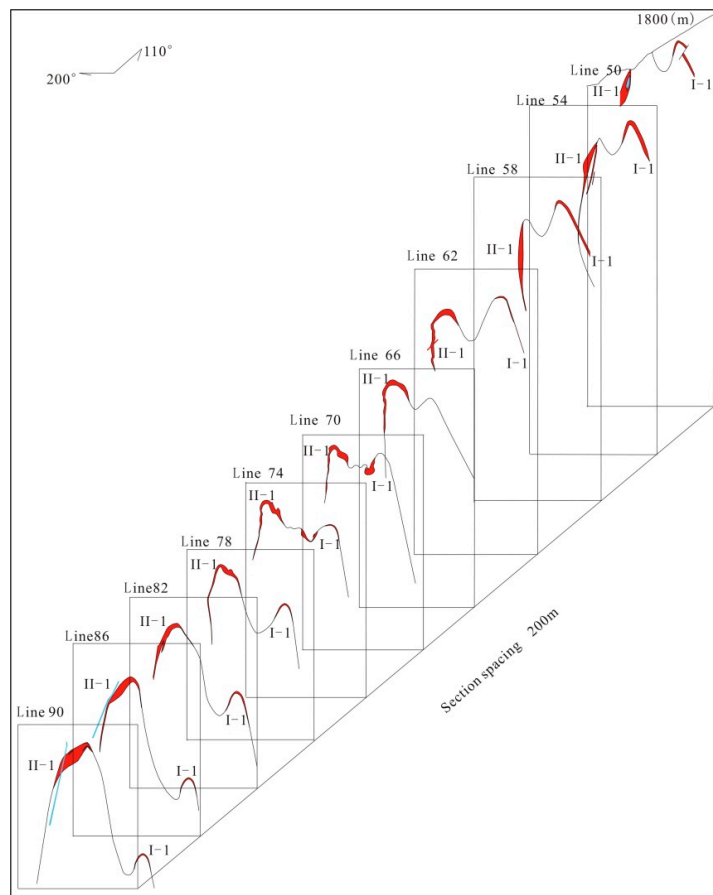

Figure 5. Joint Geological Section Map of the Qiandongshan–Dongtangzi Pb-Zn Deposit.

The No. I-1 ore body is located on both wings and the saddle of the northern secondary fold of the "M" complex anticline, and is strictly controlled by the northern secondary fold. The total length of ore body control exceeded 1700 m (402 m in the Dongtangzi ore section and 1304 m in the Qiandongshan ore section), with thicknesses ranging from 0.91 m to 9.36 m, and an average thickness of 8.14 m. The Pb grade varies from 0.17% to 3.93%, with an average of 1.21%, while the Zn grade ranges from 0.27% to 7.61%, with an average of 5.68%. The ore body is stratified and stratiform-like in shape, consistent with the common occurrences of the medium-low temperature hydrothermal lead–zinc deposit [18], and is not closed to the west. The ore body only appears on the surface (Qiandongshan ore section) with a length of approximately 550 m, but extends to a depth extension of 1350 m. The dip direction of the ore body is 288°, with an upper dip angle of 31° to 39° and a lower dip angle of 33° to 19°. The engineering control extends the ore body inclination to a maximum of 450 m. The dip direction angle of the ore body is oriented between 345° and 7°, with a dip angle of 56°–79°. The overall continuity of the ore body is good, but there is a barren section of approximately 80–150 m of silicified limestone and biogenic limestone interbedded below the elevation of 1280 m, which separates it into two sub-ore bodies.

The No. II-1 ore body is located on both wings and the saddle of the southern secondary fold of the "M" complex anticline and is strictly controlled by the southern secondary fold. The total length of ore body control is 2300 m (1400 m in the Dongtangzi ore section and 900 m in the Qiandongshan ore section), with a thickness ranging from 0.48 to 40.29 m and maximum thickness in the saddle portion. The average thickness is 12.23 m.

The Pb grade ranges from 0.21% to 4.60%, with an average of 1.44%, while the Zn grade ranges from 0.21% to 11.88%, with an average of 5.51%. The ore body is saddle-shaped in the profile, and the layered and layer-like output on the plane, which is a common form of magmatic hydrothermal ore bodies deposited in carbonate formation [18] and is also a common form of low-temperature hydrothermal lead–zinc ore body controlled by anticline structure and Si/Ca surface. The ore body extends towards the west without being enclosed by a boundary, exhibiting good continuity. Its outcropping length at the surface (in the Qiandongshan mine section) is 65 m, while its length extends to 2000 m in depth. The dip direction of the ore body is between 280° and 288°. The dip angle of the Qiandongshan ore section is between 28° and 34°, while the dip angle of the Dongtangzi ore section is between 22° and 10°. The dip angle of the II-1 ore body becomes more shallow along with the orientation of the ore body to the west. The maximum depth of the ore body by the engineering control is 475 m. The dip direction angle of the northern wing of the ore body is oriented between 0° and 19°, with a dip angle of 48°–75°, while the dip direction angle of the southern wing of the ore body is oriented between 195° and 220°, with a dip angle of 55°–88°, gradually changing from a gentle to steep inclination and ultimately reversing.

According to the exploration data, there is a transition in the proportion of reserves between the I-1 and II-1 ore bodies above an elevation of 1380 m. In the Qiandongshan ore section, the area above the elevation of 1380 m is mainly dominated by the No. I-1 ore body, which accounts for 71% of the total reserves of the entire deposit. Below 1380 m, the No. II-1 ore body gradually becomes the main ore body, where the thickness and grade begin to change. The thickness of No. II-1 ore body increased and the grade becomes higher. Below the elevation of 1080 m, the No. II-1 ore body is the major ore body, and the resource of No. II-1 ore body is more than three times that of No. I-1 ore body.

The deposit exhibits zonation of Pb, Zn-Zn, and Pb-Au from east to west on the plane of the deposit. The Pb-Zn grade decreases from east to west along the trend of the ore body and correlates closely with the variation in thickness of the ore body. The thickness and grade of the ore body at the anticline saddle are the highest and gradually decrease towards the edges until it disappears. In addition to the two main useful elements of lead and zinc, Ag, Cd, Au, and Hg are also associated with the large lead–zinc deposit of Qiandongshan–Dongtangzi, and the amount of Cd resources reaches a large scale.

3.3. Ore Characteristics and Surrounding Rock Alteration

The mineral composition of lead–zinc ore comprises sphalerite, galena, pyrite, chalcopyrite, siderite, tetradymite, pyrolusite, hematite, followed by arsenopyrite, and jamesonite. Gangue minerals include calcite, ankerite, quartz, a small amount of sericite, graphite, chlorite, montmorillonite, organic carbon, etc. The minerals' assemblages in the mining area show obvious characteristics of intermediate- to low-temperature mineralization. The microstructure of ore samples reveals the presence of banded pyrite (Figure 6a), and chalcopyrite replacing galena and sphalerite and galena replacing pyrite (Figure 6b,c).

The structure of ore mainly includes crystal structure, metasomatic structure, fragmentation structure, pressure shadow structure, followed by emulsion structure, corrosion structure, skeleton crystal structure, etc. The ore structure is mainly massive, lenticular, disseminated, and patchy, followed by vein, network vein, and strip. The ore has the structural characteristics of hydrothermal ore deposits.

The natural types of lead–zinc sulfide ore can be divided into disseminated, banded, massive, and vein type sulfide ore according to the structure and mineral combination characteristics of ores.

Overall, the degree of alteration of the wall-rocks in the mining area is relatively weak, with a limited scope of alteration influence. The alteration related to mineralization is extensively developed in the near-ore wall rocks ranging from a few centimeters to 1–2 m in the roof and floor, and could extend up to 3–4 m in the saddle zone. The alteration types are mainly silicification, pyritization, and dolomitization, followed by sericitization and graphitization. The wall-rock alteration has obvious zonation, with silicification occurring

in the central part, while the sides are mainly altered to sericite, showing characteristics of medium- to low-temperature hydrothermal alteration.
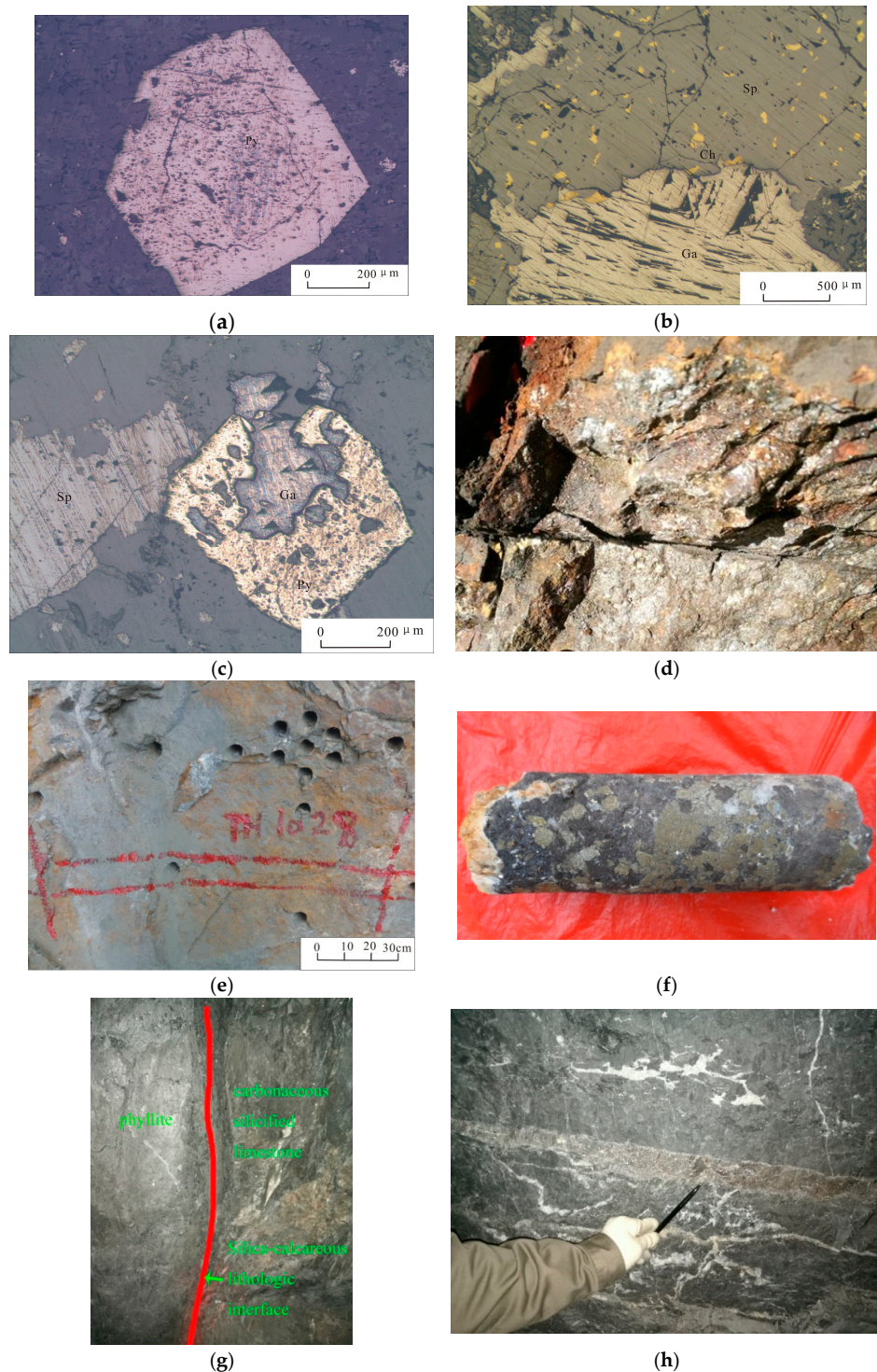
Figure 6. Outcrops and Microscopic Mineralization Characteristics of Pb-Zn Ores in the Qiandongshan–Dongtangzi Pb-Zn Deposit. (**a**) Ring-banded pyrite occurs in lead–zinc ores; (**b**) chalcopyrite replacing galena and sphalerite; (**c**) the skeleton crystal structure formed by galena metasomatism with pyrite; (**d**) Shuibogou massive sulfide outcrops. (Ag 4.5 g/t, TFe 33.69%); (**e**) Hetaogou massive sulfide outcrops (Au 10.81 g/t, Ag 3.39 g/t, TFe 31.72%); (**f**) sulfide aggregate core at 74.33 m of a borehole (Au 3.40 g/t, Ag 47 g/t, Pb 1.06%, Zn 16.5%, Cu 0.18%); (**g**) main metallogenic structural plane of lead–zinc ore body; (**h**) the Secondary metallogenic structural plane of lead–zinc ore body.

3.4. Mineralization and Metallogenic Structure

The lead–zinc ore bodies in the Fengtai orefield mainly occur in the depleted space of the contact zone between the limestone of the Gudaoling Formation and the phyllite of the Xing Formation in the anticline core. In addition, vein-like and network-like ore bodies were also found in the internal faults and fissures of limestone in the lower section of the Gudaoling Formation, such as the small-scale ore bodies in the Qiandongshan and Dongtangzi sections. In the lower member of the Xinghongpu Formation, the ore bodies occur in the interbedded fissure of phyllite, such as ore bodies in Bafangshan–Erlihe. The vein-like and layer-like ore bodies in the limestone lens body of the middle section of the Xinghongpu Formation, such as the small lead–zinc deposits in Yafangwan.

Although the magmatic rocks in the Fengtai orefield, where the large Qiandongshan–Dongtangzi lead–zinc deposit is located, are not very developed, in addition to the industrial deposits of lead, zinc, and gold, there are still a number of hydrothermal-related ore (mineralization) points, such as Jiuzigou copper (mineralization) points and Wangjialeng iron point. These iron and copper mineralizations often have a transitional relationship with the lead–zinc deposit in space, forming a metallogenic system related to magmatic hydrothermal fluid. The lead–zinc–copper polymetallic metallogenic belt of Qiandongshan–Weiziping–Tongpaigou, in which Qiandongshan–Dongtangzi Pb-Zn Deposit is located, exhibits obvious mineralization zoning: the west section of Yindongliang–Qiandongshan is mainly lead–zinc mineralization; the middle section of Tieluwan–Jiuzigou is mainly lead–zinc–copper mineralization; and the east section of Wangjiagou–Tongpaigou is dominated by copper mineralization [19]. During surface exploration around the Xiba pluton which extends eastward from the Pb-Zn-Cu polymetallic mineralization zone of Qiandongshan–Weiziping–Tongpaigou, massive sulfide mineralization was observed (Figure 6d,e). Similar rocks were also encountered in shallow drilling (Figure 6f).

The large Pb-Zn deposit is controlled by the anticlinal structure (III level) and the interface of lithology, and the ore body occurs in the contact area between Gudaoling Formation and Xinghongpu Formation. The ore-forming structure of the deposit is a fold-fault tectonic system, that is, the anticlinal and fault compound ore-forming tectonic system, which is the main form controlling the ore belt (orefield) output. Fold structure mainly controls the distribution of deep buried metallogenic geological bodies. The ore-controlling fold structure is Qiandongshan–Dongtangzi complex's anticline and its secondary anticline fold. The ore body is controlled by the WNW fold (III and IV level) and the interlayer fault zone. The anticlinal metallogenic structure and the interface between shallow metamorphic mudstone–clastic carbonate rock formations together form the geochemical barrier for mineralization in the mining area. The main metallogenic structural plane is the lithologic contact interface of Gudaoling Formation limestone and Xinghongpu Formation phyllite, namely the silica–calcium plane (Figure 6g). The secondary structural plane is the fractures in limestone and phyllite near the contact zone (Figure 6h). The main ore bodies occur in the interbedded tectonic belt within the contact zone between the limestone of Gudaoling Formation and the phyllite of Xinghongpu Formation in the saddle part of anticline and the extension part of the two wings. The direct ore-bearing rocks are silicified limestone, silicified phyllite, and quartz veins. The ore body is deposited to the west, the surface section of the surface is stratiform in the plane and section, and the hidden section is parabolic. In the interlayer, faults and fissures locally developed in limestone and phyllite near the contact zone, and there are vein-shaped secondary ore bodies formed by hydrothermal filling. They are controlled by faults, and their scale is generally small, which is a manifestation of the surface ore-controlling characteristics of secondary faults formed by regional tectonic movements.

4. Geochemical Anomaly Characteristics

The 1:50,000 geochemical exploration dispersive flow and stream sediments of the Qiandongshan–Dongtangzi lead–zinc deposit show that seven elements of Pb, Zn, Ag, Au, As, Hg, and Sb are enriched in the area, followed by Cu and Bi relatively enriched,

while eight elements of Ni, Co, Cr, V, Mn, Ti, Mo, and B are relatively depleted. The anomalous element combination of Pb-Zn-Ag-Cu-Au-As-Hg has obvious characteristics of hydrothermal lead–zinc deposit, and the anomalous element combination is basically consistent with the typical hydrothermal lead–zinc deposit in the southeast Guizhou Province [20].

5. Geochemical Characteristics of Deposits

5.1. Pyrite Genesis

The electron probe analysis of the ore samples in the Qiandongshan–Dongtangzi lead–zinc deposit is shown in Table 1. The analysis results of the samples showed that the $\omega(Co)/\omega(Ni)$ values of pyrrhotite were in the range of 4.44 to 15.57, with an average of 8.56. The $\omega(Co)/\omega(Ni)$ values of the vein lead–zinc ore were in the range of 8.25 to 29.20, with an average of 18.70. In the discrimination diagram of Co/Ni ratio, the plots are all located near the evolution line of $\omega(Co)/\omega(Ni) = 10$, far exceeding the evolutionary line of $\omega(Co)/\omega(Ni) = 1$. This indicates that it is a magmatic–hydrothermal–origin pyrite [21]. The content of As, Co, and Ni in pyrite are important indicators for determining the genesis of pyrite and distinguishing ore deposit types [22]. In the As-Co-Ni ternary phase diagram, the plots are all located in the volcanic–magmatic–hydrothermal origin area, indicating that pyrite in lead–zinc ores has a volcanic–magmatic–hydrothermal origin.

Table 1. Electron Microprobe Analysis Results of Pyrite in the Qiandongshan–Dongtangzi Pb-Zn Deposit.

Sample Type	Number of Samples	w(Fe)/ %	w(S)/ %	w(Pb)/ 10^{-6}	w(As)/ 10^{-6}	w(Co)/ 10^{-6}	w(Ni)/ 10^{-6}	w(Cu)/ 10^{-6}	w_{total}/ %
Massive ore pyrite	6	46.55	53.31	440.00	3441.67	750.00	41.67	131.67	100.34
The veined ore pyrite	6	46.21	52.69	941.67	7971.67	778.33	21.67	745.00	99.94

Note: Data from [17]; w(.) is the content of elements or compounds; w_{total} indicates the total content.

Previous studies have conducted a statistical analysis on the content of trace elements in sphalerite and pyrite from two types of deposits, i.e., stratiform and hydrothermal type [23,24]. The values obtained from the analysis can be used to distinguish the genetic type of the deposit: The stratiform lead–zinc deposits are characterized by $\omega(Ga) > 30 \times 10^{-6}$, $\omega(Zn)/\omega(Cd) > 300$, and $\omega(Co)/\omega(Ni) < 1.5$, while the hydrothermal lead–zinc deposits exhibit $\omega(Ga) < 40 \times 10^{-6}$, $\omega(Zn)/\omega(Cd) < 300$, and $\omega(Co)/\omega(Ni) > 1.5$. The average content of Ga elements in the ore samples of the Dongtangzi lead–zinc deposit is 13.23×10^{-6}, the average content of $\omega(Zn)/\omega(Cd)$ is 14.65, and the average content of $\omega(Co)/\omega(Ni)$ is 6.17, which also probably proves that the Qiandongshan–Dongtangzi lead–zinc deposit is of magmatic–hydrothermal origin.

5.2. Geochemical Characteristics of Elements

5.2.1. Geochemical Characteristics of Trace Elements

Statistical analysis shows that the Sb content of ore from the Dongtangzi ore section, the Qiandongshan ore section, the Fengya ore section, the Yindongliang ore section, and the Bafangshan–Erlihe lead–zinc mining area ranges from $(9.7–35) \times 10^{-6}$, while the As $(29.1–135.5) \times 10^{-6}$, the Hg $(8.22–135) \times 10^{-6}$, and the Cd $(815–>1000) \times 10^{-6}$ (Table 2) [17,25]. Among them, the content of Sb, Hg, and Cd in lead–zinc ore is significantly higher than that of phyllite, which is two~three orders of magnitude higher than of silicified/mineralized limestone, Furthermore, it is far higher than the average abundance of sedimentary rocks [26]. Since Sb is an indicator element for hydrothermal activity, it indicates that ore-forming materials may be enriched through the hydrothermal process. The content of elements such as, Ag, As, and Bi related to magmatic–hydrothermal activity are significantly higher in lead–zinc ores, reflecting strong hydrothermal activity during mineralization [5]. The content of W and Mo in lead–zinc ore and mineralized limestone are significantly higher than those in bioclastic limestone. These elements, including W,

Mo, As, Sb, Hg, Bi, and Cd are indicator elements of magmatic–hydrothermal activity. The contents of W, Mo, As, Sb, Hg, Bi, and Cd in lead–zinc ore are significantly higher than those in surrounding rocks, indicating a close correlation between magmatic–hydrothermal activity and the lead–zinc mineralization process.

Table 2. Analysis Results of Trace Elements and REE of different Rock types and ore in the Fengtai orefield.

	Dongtangzi Lead Zinc Deposit					Bafangshan—Erlihe Lead—Zinc Deposit				Xiba Pluton			
Number of Samples	3	3	2	2	4	9	2	1	8	3	3	3	3
Lithology	Rock1	Rock2	Rock3	Rock4	Rock5	Rock6	Rock1	Rock7	Rock5	Rock8	Rock9	Rock10	Rock11
Au							0.34	0.035	0.038				
Ag							10.57	0.04	0.04				
As							135.5	0.20	0.39				
Cd	682.7	2.37	0.95	0.85	0.15								
Bi							8.22	0.39	3.87				
Cr	4.67	4.03	9.45	7.15	103.6								
Co	51.03	2.53	4.70	16.55	21.80								
Ni	8.27	23.70	9.60	8.70	42.85								
Cu	298.7	3.93	47.45	68.25	15.23								
Zn	>10,000	156.7	12,757	54,050	75.25		222.0	38.00	320.0				
Ga	13.23	0.77	2.40	3.40	22.30								
Rb	6.73	6.03	10.75	8.40	221.2					106.0	74.43	127.3	172.3
Sr	19.67	344.3	85.30	36.95	97.95					724.3	701.7	542.7	332.3
Mo	0.37	2.53	4.60	4.30	0.38					0.18	0.59	0.77	0.24
Cd	682.7	2.37	0.95	0.85	0.15								
In	0.20	0.50	58.15	183.0	0.10								
Sb	9.70	0.00	0.00	0.00	3.55		27.10	0.28	0.06				
Hg							8.22	0.02	0.03				
Ba	250	0.50	0.95	0.75	720.9					1344.3	227.7	419.7	880.7
W	4.20	0.87	3.35	4.30	4.45								
Tl	0.10	0.10	0.15	0.30	1.00					3552.7	5566	5047.7	1281
Pb	6422	149.8	1387	36,945	53.30		250.5	9.93	38.70				
La	0.87	2.23	1.65	1.60	42.88	20.77	22.05	25.00	127.2	30.03	24.37	31.57	38.30
Ce	1.40	3.70	3.15	2.95	75.03	38.20	46.40	56.10	267.1	50.28	46.60	57.80	65.03
Pr	0.17	0.53	0.45	0.40	9.28	4.35	4.87	6.17	29.70	6.08	5.95	6.94	7.44
Nd	0.73	1.93	2.10	1.85	33.65	15.63	19.20	23.3	107.4	20.33	23.67	25.77	25.03
Sm	0.13	0.40	0.70	0.60	4.95	3.01	3.59	4.57	20.53	3.39	4.53	4.56	4.05
Eu	0.07	0.10	0.15	0.10	1.03	0.60	1.04	1.09	4.00	1.35	1.26	1.19	1.21
Gd	0.13	0.37	0.60	0.50	4.63	2.39	3.84	4.69	14.84	3.00	3.87	4.09	3.58
Tb	0.03	0.10	0.15	0.15	0.63	0.35	0.54	0.71	1.96	0.42	0.62	0.60	0.48
Dy	0.23	0.47	0.90	0.90	3.10	2.53	2.98	3.73	11.90	2.13	3.44	3.24	2.31
Ho	0.07	0.10	0.20	0.20	0.73	0.38	0.56	0.76	1.60	0.46	0.78	0.73	0.47
Er	0.17	0.27	0.50	0.55	2.23	1.17	1.77	2.28	5.16	1.20	2.10	1.98	1.43
Tm	0.00	0.03	0.10	0.15	0.40	0.16	0.25	0.37	0.81	0.21	0.35	0.33	0.21
Yb	0.23	0.30	0.55	0.70	2.73	1.05	1.70	2.28	6.03	1.36	2.27	2.15	1.43
Lu	0.00	0.00	0.10	0.10	0.45	0.16	0.23	0.33	0.95	0.21	0.35	0.34	0.23
Y	1.57	2.53	4.60	4.30	19.78					12.63	21.93	20.83	13.93
REE	4.23	10.47	11.3	10.75	181.8	90.74	109.0	131.4	599.1	120.5	120.2	141.3	151.2
LREE	3.37	8.87	8.20	7.50	166.9		97.14	116.2		111.5	106.4	127.9	141.1
HREE	0.86	1.57	3.10	3.25	14.83		11.86	15.15		8.99	13.78	13.46	10.14
LREE/HREE	3.92	5.53	2.65	2.31	11.58	3.91	8.19	7.67	5.01	12.40	7.72	9.50	13.91
$(La)_N/(Yb)_N$	2.73	5.53	2.10	2.10	11.70	20.38	10.56	10.99	21.40	15.96	7.72	10.64	19.16
δEu	1.00	0.53	0.75	0.60	0.65	0.68	0.94	0.72	0.66	1.28	0.90	0.83	0.96
δCe	0.90	0.87	0.90	0.90	0.90	0.93	1.06	1.06	1.01				

Note: Element content unit is 10^{-6}; Dongtangzi data came from [17]; the data of Bafangshan–Erlihe came from [25]; Xiba rock mass data from [27]; Rock1 is Lead–Zinc ore; Rock2 is Bioclastic limestone; Rock3 is Silicified limestone; Rock4 is Mineralized Silicified limestone; Rock5 is Phyllite; Rock6 is Limestone; Rock7 is Mineral-bearing siliceous rock; Rock8 is Granodiorite; Rock9 is Quartz diorite; Rock10 is Monzonite diorite; and Rock11 is Monzogranite.

The sphalerite in the lead–zinc ore of Dongtangzi ore section is relatively rich in Sn, W, Co, and Ni elements. Sn and W are highly active elements during magmatic–hydrothermal processes, indicating that mineralization is closely related to hydrothermal activities [28]. The galena in the Bafangshan–Erlihe lead–zinc deposit has high contents of Ag, Sb, Bi, and Se. The amounts of Au, Pt, and Pd in the ore samples are much higher than the

crustal average, with a Pt/Pd ratio of 0.34–0.58, which is less than the crustal average value (Pt/Pd = 1). This observation indicates that late-stage hydrothermal activities were relatively intense [25]. The enrichment characteristics of these elements are consistent with the development of quartz and calcite veins formed in the deposit.

On the spider diagram for primitive mantle normalized trace elements (Figure 7), lead–zinc ores and mineralized rocks have similar trace element patterns with granodiorite, quartz diorite, quartz monzonite diorite, and monzonite granite of Xiba pluton, all of which are right-trending. Except for the lead–zinc ores of the Dongtangzi section, the elements in all samples were higher than those in the primitive mantle. The rocks were obviously enriched in large ion lithophile elements such as Rb and relatively depleted in Ti and Ba. The depletion of Ti was caused by the separation and crystallization of plagioclase in the magma, while the depletion of Ba was a result of the residual state of granitic magma. In general, the enrichment characteristics of trace elements in the Qiandongshan–Dongtangzi Pb-Zn deposit are highly similar to those of the Xiba pluton, indicating that this deposit is associated with magmatic–hydrothermal fluids.
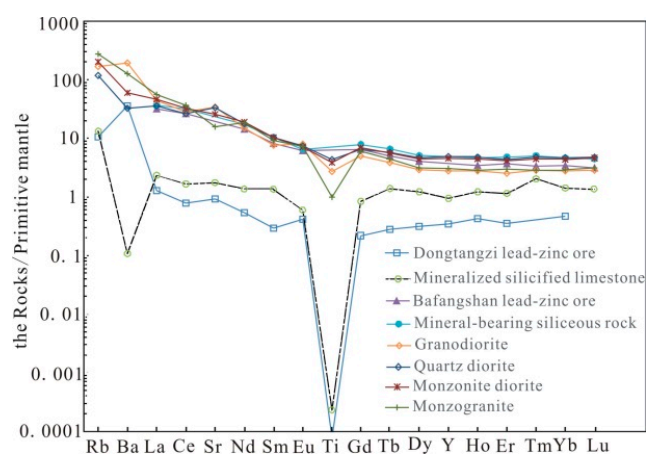

Figure 7. Chondrite-normalized rare earth element and other elements patterns of the Qiandongshan–Dongtangzi rocks.

5.2.2. Geochemical Characteristics of Rare Earth Elements

The average content of total rare earth elements in phyllite from the Dongtangzi ore section is 181.46×10^{-6}, with a LREEs/HREEs ratio of 11.59. LREEs are enriched and there is significant fractionation of rare earth elements, with a negative anomaly of Eu (0.65) and a weak negative anomaly of Ce (0.93). The mean value of the total REE content in bioclastic limestone is 10.47×10^{-6}, with a ratio of LREEs/HREEs is 5.53. LREEs are enriched and there is significant fractionation of rare earth elements, with a negative anomaly of Eu (0.53) and a weak negative anomaly of Ce (0.87). The mean value of the total REE content in silicified limestone is 11.28×10^{-6}. The Eu exhibits a negative anomaly with a value of 0.75, while Ce shows a weak negative anomaly with a value of 0.89. The total content of rare earth elements, as well as the fractionation of light and heavy rare earth elements, in ore-bearing silicified limestone is similar to that in silicified limestone. However, the negative anomaly of Eu in ore-bearing silicified limestone is more prominent. The content of total rare earth elements in lead–zinc ores is 4.33×10^{-6}, with a ratio of LREEs/HREEs is 3.61. The fractionation of light and heavy rare earth elements is small, with an average value of Eu anomaly at 0.97 and Ce anomaly at 0.88. [17]. The composition of rare earth elements suggests that lead–zinc ore is more closely related to hydrothermal origin, and these characteristics are basically consistent with the characteristics of rare earth elements in the Bafangshan–Erlihe mining area [25] (Wang, 2011).

The chondrite normalized REE partition patterns of Pb-Zn ores, ore-bearing siliceous rocks, and Xiba granodiorite, quartz diorite, monzonite diorite, and monzonite granite are very similar (Figure 8), indicating that they have the same material source, all of which are

related to magmatic–hydrothermal fluid. The rare earth element model is characterized by enrichment in light REE, showing no Eu anomaly and negative Ce anomaly, indicating that it is not the product of normal seawater deposition. Furthermore, it also shows a distinct difference in positive Eu anomaly characteristics compared to near-source sulfide ores and volcanic rocks in typical submarine hydrothermal sedimentary deposits [29,30]. There are significant differences in the rare earth element patterns between limestone and other types of rocks, indicating different sources of materials. The rare earth element patterns in lead–zinc ores exhibit weak Eu anomalies, suggesting that they are not the products of normal seawater sedimentation [31]. Additionally, the significant differences in the Eu positive anomaly characteristics between lead–zinc ores and seafloor hydrothermal sedimentary rocks indicate that lead–zinc ores are of hydrothermal origin.
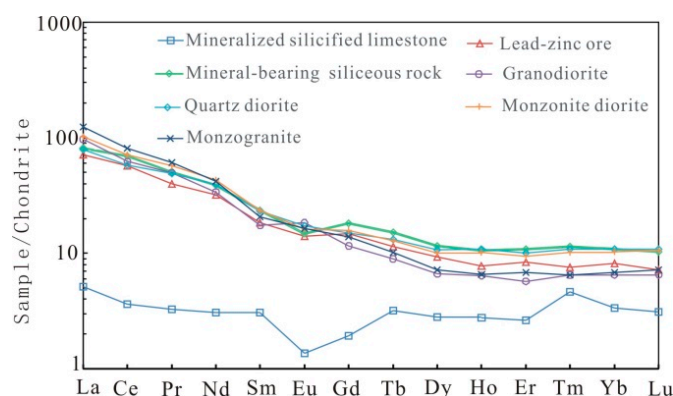

Figure 8. Chondrite REE patterns of the Qiandongshan–Dongtangzi rocks.

5.3. Isotopic Geochemical Characteristics

5.3.1. H-O Isotopic Composition

Studies on hydrogen and oxygen isotopes of the Qiandongshan–Dongtangzi lead–zinc deposit (Table 3) suggests that the ore-forming fluids were mainly derived from magmatic water in the early stage, and later mixed with groundwater and atmospheric water [17] (Figure 9). The hydrogen and oxygen isotopic ratios of 37 quartz samples from Bafangshan–Erlihe Pb-Zn deposit (the Jianduduananshan–Bafangshan–Erlihe lead–zinc polymetallic ore belt in which the Bafangshan–Erlihe lead–zinc deposit is located is 12 km apart from the Qiandongshan–Shuibaigou lead–zinc ore belt in which the Dongtangzi–Qiandongshan lead–zinc deposit is located.) in the Fengtai orefield are all in the area of magmatic water and organic water, it is considered that the ore-forming fluids have the characteristics of multiple sources. And the $\delta^{18}O_{H2O}$ ratio ranges are close to the range of magmatic water defined by Ohmoto (1986) [32], which reflects the contribution of magmatic water during the mineralization process [6]. The δD values in two sphalerite samples and five quartz samples in the Bafangshan–Erlihe lead–zinc deposit indicate a mixing characteristic of atmospheric water and magmatic water, suggesting that ore-forming fluids were of mixed origin [25]. The results of hydrogen–oxygen isotope studies on the Yafangwan lead–zinc deposit in the southern limb of the Changgou–Donggou anticline in the Fengtai orefield indicate that the ore-forming fluids were a mixture of magmatic water and metamorphic water. The high homogenization temperature of fluid inclusions may be related to the intrusion of the Xiba pluton [33]. The ore-forming fluid in the main ore-forming stage of the magmatic hydrothermal lead–zinc deposit has the characteristics of a mixture of atmospheric water and magmatic water [18]. The hydrogen and oxygen isotopic composition characteristics of the lead–zinc deposit in the Fengtai orefield indicate that the main component of the ore-forming fluid lie between metamorphic and formation water, while the participation metamorphic water and atmospheric water are in the later stage. This fully indicates that the lead–zinc deposit in the Fengtai orefield

is likely of magmatic–hydrothermal origin, which is consistent with the extensive outcrops of Indosinian granites in the orefield.

Table 3. H-O Isotopic Compositions of Pb-Zn Ores in the Fengtai orefield.

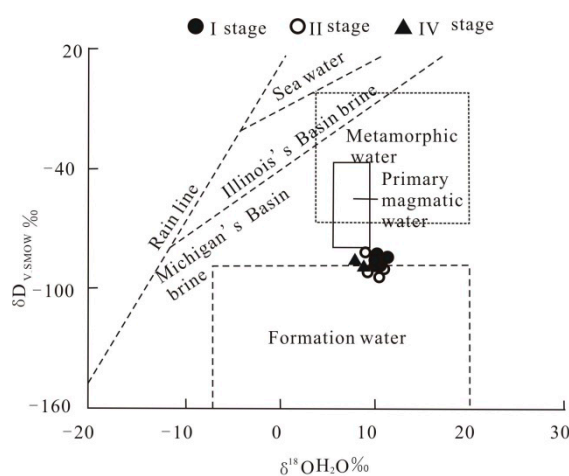| Name of Mine	No.	Number of Amples	Mineral	$\delta D/‰$	$\delta^{18}O/‰$	T/°C	$\delta^{18}O_{H2O}/‰$	References
Dongtangzi	1	7	quartz	−87.91	20.56	215.00	9.76	[17]
	2	5	quartz	−86.26	20.72	225	10.52	
	3	4	quartz	−86.13	20.50	200.00	8.80	
	average	16	quartz	−86.77	20.59	213.33	9.69	
Bafangshan–Erlihe	4	37	quartz	−87.49	18.89	218.95	8.31	[6]
Qiandongshan	5	5	quartz	−94.2			−13.04	[34]
	6	3	quartz	−82			−10.56	[1]

Figure 9. Diagram of $\delta D_{V\text{-SMOW}}$-$\delta^{18}O_{H2O}$ in Qiandongshan–Dongtangzi Pb-Zn Deposit.

In conclusion, numerous H-O isotope data indicate that the source of ore-forming fluid is closely related to magmatism and metamorphism, which is also consistent with the magmatism and metamorphism the Fengtai orefield during the Indosinian period.

5.3.2. Sulfur Isotope Characteristics

The $\delta^{34}S$ values of sulfides in Sedex-type lead–zinc deposit often exhibit a large range of variation, with most falling within the interval of 20‰–30‰ [1]. In contrast, the $\delta^{34}S$ values of lead–zinc deposits associated with magmatic activity are generally small and vary from −5‰ to 10‰ (Table 4). The $\delta^{34}S$ values of sulfides from the Qiandongshan–Dongtangzi lead–zinc deposit range from 4.29‰ to 9.63‰. The $\delta^{34}S$ values of sulfides in the Qiandongshan–Dongtangzi lead–zinc deposit have smaller and homogeneous ranges, all of which are less than 10‰. These characteristics are significantly different from those of the Sedex-type lead–zinc deposits with larger $\delta^{34}S$ value ranges. However, they share similarities with the $\delta^{34}S$ values of lead–zinc deposits related to magmatic activities, such as Dongzhongla, Tibet, and Qixiashan, in the Jiangsu Province. These $\delta^{34}S$ values indicate that the Qiandongshan–Dongtangzi lead–zinc deposit was probably formed by magmatic–hydrothermal processes and suggest that magmatic activities in the region played a role in mineralization.

Table 4. Sulfur Isotope Compositions of the Qiandongshan–Dongtangzi Pb-Zn Deposit.

Type of Deposit	Ore Deposit	Number of Samples	δ^{34}S	References
Sedex type	Huogeqi lead–zinc deposit in langshan area, neimenggu Province		3.6‰~23.5‰	[35]
	Jiashengpan lead–zinc deposit		17‰~31.4‰	[36]
	Dongshengmiao lead–zinc deposit		21.7‰~41.84‰	[37]
	Changba lead–zinc mine in Gansu Province		11.4‰~27.81‰	[12]
Magmatic hydrothermal type	Dongzhongla lead–zinc deposit in Tibet		2.2‰~4.8‰	[38]
	Qixiashan lead zinc–deposit, Jiangsu Province		−4.6‰~3.8‰	[37]
	Dongtangzi mine section	14	4.29‰~9.63‰	[17]
	Qiandongshan mine section	11	5.25‰~9.35‰	[39]
	Bafangshan–Erlihe	57	3.70‰~12.90‰	[6]
	Shoubanya–Yindongliang	6	2.3‰~8.0‰	[40]

The sulfur isotope results of sulfides from the Qiandongshan–Dongtangzi deposit show that the sulfur δ^{34}S value is much lower than that of global Devonian seawater, with the minimum value in the Middle Devonian being 17‰, which may indicate the addition of magmatic sulfur [6]. Wang et al. [25] argue that the sulfur isotopic composition of the Bafangshan–Erlihe Pb-Zn deposit is different from both magmatic hydrothermal deposit and sedimentary deposit, showing characteristics of mixed sulfur sources. The vein-like and disseminated sphalerite and pyrite within the diorite porphyrite dikes in the Bafangshan–Erlihe Pb-Zn deposit has typical characteristics of magmatic sulfur, providing direct evidence that magmatic activity contributes to some of the sulfur source.

5.3.3. Lead Isotope Characteristics

The Pb isotope compositions of the main lead–zinc deposits in the Fengtai orefield are shown in Table 5. The ^{206}Pb/^{204}Pb ratios of each ore deposits range from 18.02 to 18.14, the ^{207}Pb/^{204}Pb ratios range from 15.60 to 15.71, and the ^{208}Pb/^{204}Pb ratios range from 38.07 to 38.50. The Pb isotope ratios of individual lead–zinc deposit in the mining area are very stable, with a variation range generally less than 1%. The Pb isotopic composition of the largest Xiba granite in the mining area is 17.77–17.94 for ^{206}Pb/^{204}Pb, 15.47–15.52 for ^{207}Pb/^{204}Pb, and 37.85 ~ 37.89 for ^{208}Pb/^{204}Pb. It is evident that the Pb isotopic compositions of the Fengtai Pb-Zn deposits and the Xiba pluton are quite similar, suggesting that the various ore deposits in the Fengtai orefield and the Xiba pluton have the same lead source. This suggests a close relationship between mineralization of lead–zinc ore deposits in the Fengtai and magmatic activity.

Table 5. Lead isotope compositions of Pb−Zn deposits in Fengtai orefield.

No.	Location	Number of Samples	Mineral	^{206}Pb/^{204}Pb	^{207}Pb/^{204}Pb	^{208}Pb/^{204}Pb	References
1	Dongtangzi	10	Galena	18.14	15.71	38.50	[17]
2	Qiandongshan	11	Galena	18.06	15.61	38.15	[39]
3	Bafangshan—Erlihe	9	Galena	18.08	15.63	38.34	[25]
4	Fengya	4	Ore	18.09	15.61	38.27	[24]
5	Shoubanya	6	Ore	18.02	15.60	38.07	[34]
6	Yindongliang	5	Ore	18.11	15.67	38.33	[41]
7	Xiba pluton	1	Quartz diorite	17.94 ± 29	15.47 ± 25	37.85 ± 64	[42]
		4	Potassium feldspar	17.77	15.52	37.89	[41]

The results show that the Pb isotopic composition of sulfides in the Pb−Zn deposits in the Fengtai orefield mainly falls within the upper crust and mantle mixing zone (magmatism) on the Δβ-Δγ diagram, indicating that the Pb source of the ore may be the mixture of

mantle-derived lead and upper crust lead (Figure 10). This suggests that the ore deposit formed in a tectonic environment transitioning from a subduction zone to an orogenic belt, rather than a hydrothermal sedimentary environment, indicating that magmatic activity originating from crust-mantle interactions may have provided some of the ore-forming elements [6,39].
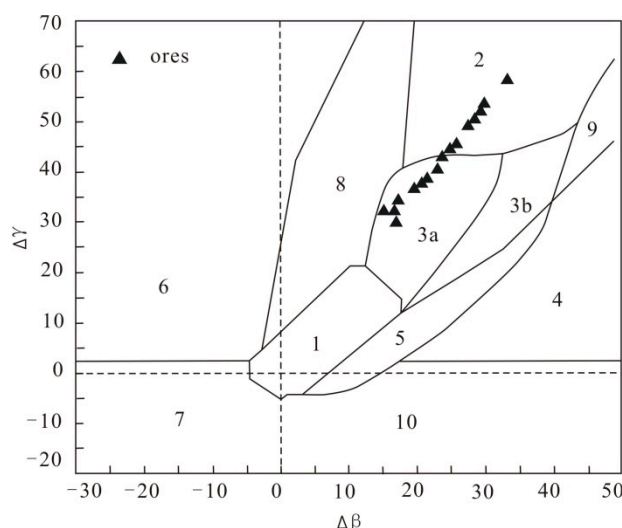

Figure 10. $\Delta\beta$-$\Delta\gamma$ genetic discriminate diagram of galena from the Fengtai orefield (after [41]). 1—Lead sourced from mantle; 2—Lead sourced from upper crust; 3—Subducting lead sourced from upper crust and mantle (3a—magmatism; 3b—sedimentation); 4—Lead of chemical deposition; 5—Lead of submarine hot-water; 6—Mesometamorphism; 7—Lead of kata-metamorphism; 8—Lead of orogenic belt; 9—Lead of upper crust in ancient shale; 10—Lead of retrograde metamorphism.

5.4. Metallogenic Age

The understanding process of the formation age of lead–zinc deposits in the Fengtai orefield can be divided into two stages. The first stage, before 2011, involved a viewpoint attributing the lead–zinc deposits within the region to a volcanogenic sedimentary origin. As a result, it was indirectly considered that the period of mineralization was consistent with the period of rock formation, specifically during the Middle –Late Devonian period [1,40]. Another viewpoint suggests that it is a sedimentary metamorphic type. The early sedimentation represents the lithification stage of the surrounding rock, and the later metamorphism occurred during the Indosinian period [12,43,44]. The second stage is after 2011, when isotopic dating results showed that the mineralization age of the lead–zinc deposits in the Fengtai orefield mainly ranged from 226–212 Ma, leading many scholars to have a relatively unified understanding that the mineralization age of these lead–zinc deposits belongs to the Late Triassic period (Table 6).

Table 6. Isotopic Age Data of Ore and Igneous Rock Samples from the Fengtai orefield.

	Location	Test Sample	Test Method	Age	References
1	Bafangshan—Erlihe lead—zinc deposit	pyrite	Re-Os isochron	226 ± 17 Ma	[45]
2	Bafangshan—Erlihe lead—zinc deposit	sphalerite	Rb-Sr isochron	220.7 ± 7.3 Ma	[46]
3	Bafangshan—Erlihe lead—zinc deposit	pyrite	Re-Os isochron	226 ± 17 Ma	[47]
4	Qiandongshan–Dongtangzi lead—zinc deposit	Sphalerite, galena, pyrite	Rb-Sr isochron	211.6 ± 2.6 Ma 215.3 ± 3.2 Ma	[6]
5	Changba—Lijiagou lead—zinc deposit	sulfide	Rb-Sr isochron	222.3 ± 2.2 Ma	[48]
	average			220.3 ± 6.55 Ma	
6	Bafangshan—Erlihe lead—zinc deposit	Diorite porphyrite veins	Zircon U-Pb	214 ± 2 Ma	[45]
7	Bafangshan—Erlihe lead—zinc deposit	Diorite porphyrite veins	Zircon U-Pb	221 ± 3 Ma	[45]
8	Bafangshan—Erlihe lead—zinc deposit	Diorite porphyrite veins	Zircon U-Pb	214 ± 2 Ma	[25]

Table 6. *Cont.*

	Location	Test Sample	Test Method	Age	References
9	Bafangshan—Erlihe lead—zinc deposit	Granite porphyry dikes	Zircon U-Pb	217.9 ± 4.5 Ma	[25]
10	Bafangshan—Erlihe lead—zinc deposit	Diorite porphyrite veins	Zircon U-Pb	220 ± 2.5 Ma	[47]
11	Dongtangzi lead—zinc deposit	Granite porphyry dikes	Zircon U-Pb	221.8 ± 1.1 Ma	[16]
12	Dongtangzi lead—zinc deposit	Granite porphyry dikes	Zircon U-Pb	226.7 ± 1.2 Ma	[16]
13	Dagou pluton	Diorite porphyrite veins	Zircon U-Pb	225.0 ± 1.0 Ma	[16]
	Dagou pluton	Granodiorite dikes	Zircon U-Pb	217.4 ± 2.0 Ma	[16]
14	average			219.8 ± 2.14 Ma	
15	Duji pluton	Biotite granite	Zircon U-Pb	223.7 ± 1.0 Ma	[16]
16	Xiba pluton	monzogranite	Zircon U-Pb	219 ± 1 Ma	[47]
17	Xiba pluton	granodiorite	Zircon U-Pb	218 ± 1 Ma	[47]
18	Xiba pluton	monzogranite		214.9 ± 1.1 Ma	[49]
19	Hejiazhuang pluton			248 ± 2 Ma	[50]
20	Hejiazhuang pluton	granodiorite	LA-ICP-MS	246 ± 3 Ma	[51]
21	Hejiazhuang pluton	granodiorite	LA-ICP-MS	248 ± 2 Ma	[50]
22	Huahongshuping pluton	granodiorite	Zircon U-Pb	214.3 ± 2.7 Ma	[7]
23	Huahongshuping pluton	granodiorite	Zircon U-Pb	225.3 ± 1.4 Ma	[16]
24	Taibai pluton			216 Ma	[52]
25	Taibai pluton	Biotite monzogranite		214 ± 2 Ma	[53]
26	Baoji pluton			216~210 Ma	[51]
27	Huayang Rock mass	monzogranite	LA-ICP-MS	214 ± 2 Ma	[54]
	average			224.4~225.1 ± 1.94 Ma	

　　　The Fengtai orefield is extensively developed with magmatic rocks, such as the largest Xiba pluton and Huahongshuping pluton. The granite plutons have concentrated ages of 248–214 Ma [55], and the granite dikes have concentrated ages of 226–214 Ma [55]. The dating results show that the magmatic activity of the Fengtai orefield occurred in the Late Triassic period, and its formation age roughly corresponds to the mineralization age of lead–zinc deposit.

　　　Wang et al. [8] proposed that the Devonian carbonate and clastic rocks in the Fengtai orefield are sedimentary products of the littoral-shallow sea facies in the foreland basin, formed under compression environment. This mineralization dynamic background is completely different from the typical Sedex Pb-Zn deposits. Therefore, the Devonian period in the Fengtai orefield is not suitable for hydrothermal sedimentation or SEDEX mineralization, and the Pb-Zn deposits are products of large-scale tectonic deformation, metamorphism, magmatism, and fluid activity in the collision stage of the Qinling orogenic belt after the Late Triassic period.

　　　In summary, the geochronology data of the Fengtai orefield show that the mineralization age of Pb-Zn deposit is concentrated in 226–211 Ma. The emplacement of granite dikes and Pb-Zn deposit appears to be roughly equivalent to the formation age of the lead–zinc deposits (Figure 11), while the granite pluton formed slightly earlier than the granite dikes and lead–zinc deposits. The lead–zinc mineralization activity occurred slightly later than the magmatic activity in the region, and the lead–zinc deposits likely formed during the Late Triassic period.

Figure 11. Distribution map of diagenetic and metallogenic ages in the Fengtai orefield.

6. Ore Genesis and Prospecting Model

6.1. Ore Genesis

We carried out the project of "Prospecting and Prediction of FengTai" orefield on the typical lead–zinc deposits. Combined with the analysis of isotopic ages and trace element data, it is suggested that the Qinling Orogenic Belt was in the post-collision extensional stage after collision during the Indosinian period. Intense magmatic activity and mineralization occurred in this tectonic setting [13,27,56–59], which formed the basis for the formation of the Qiandongshan–Dongtangzi lead–zinc deposit. It shows obvious difference from typical Sedex lead–zinc deposit in the geological characteristics, the macroscopic and microscopic structural of lead–zinc ores, H-O-S-Pb isotopes, trace and rare earth element characteristics, mineralization age, and the relationship between ore body and granite, but they are closely related to magmatic–hydrothermal processes. In addition, there are developed skarnified minerals such as tremolite, chlorite, and biotite in the Yafangwan deposit. Silicification, ferrodolomitization, ferrocalcite, pyritization, marbleization, and sericiization are developed in the hanging wall and footwall of the main ore bodies of the Yafangwan deposit, and these characteristics show the close relationship between Pb-Zn mineralization and magmatic activity.

During the Devonian period, the Fengtai orefield was situated in an active continental margin sedimentary environment. Stable isotope studies have shown that the initial enrichment of ore-forming materials in the strata constitutes the foundation of final mineralization [6]. In the Late Indosinian period, the high-temperature, acidic and lead-zinc-chloride-rich supercritical fluid exsolved from the intermediate-acidic intrusions exhibits along channels formed by WNW-trending faults, driven by structural stress and temperature gradients, and diagonally progressing from SE to NW. Organic matter often forms stable complexes with lead, zinc, and other metals in intermediate- to low-temperature hydrothermal fluids, which facilitates the transportation of ore-forming metals. Among them, the lead complexing ability is several orders of magnitude higher than that of Cl^- and CO_3^{2-} [60], and organic lead complexes make a significant contribution to the transport of lead [61,62]. The solubility of sphalerite is several times to tens of times higher in fluid media containing organic compounds compared to those without organic compounds [63]. During upward migration, the fluid extracted a large amount of SiO_2 when passing through sandstone and siltstone [18], and when entering carbonate rocks, $CaCO_3$ was converted into Ca^{2+} and HCO^{3-} that dissolved in the fluid, releasing HO^- ions, causing the fluid to shift towards alkalinity and leading to the precipitation of a large amount of SiO_2. As pH increased, the solubility of lead and zinc chloride complexes decreased by two orders of magnitude with each a one-unit increase in pH. As the pressure and temperature decrease and water–rock reactions occur, the stability of metal elements migrating in the form of chloride complexes is greatly reduced [64]. They are then converted into hydrosulfide complexes and begin to precipitate in large quantities due to the

decrease in solubility with increasing pH, eventually forming sulfide minerals of lead and zinc. The ore-forming metals suffered the metasomatism mineralization near the acid-base geochemical barrier (the Si/Ca interface), especially in the saddle detachment part of the anticline and the limb contact zone. Mineralization results in ore bodies occurring on the side of carbonate rocks [18]. According to the study results of Tagirov and Seward [64,65] and Ye Tianzhu et al. [18] on the transport conditions of zinc, the overall zinc grade of the lead–zinc ore body in the mining area is generally higher than that of lead, which may be caused by the difference in the transport effects of chloride complexes on lead and zinc in the ore-forming fluid.

Ye et al. [18] concluded that the metallogenic geological bodies of magmatic–hydrothermal origin lead–zinc deposits are intermediate-acidic intrusions, with various lithology including quartzite diorite, plagioclase granite porphyry, granite porphyry, granodiorite porphyry, granite, and quartz porphyry. Examples of such deposits include the Mengentaolegai Pb-Zn-Ag deposit in the Neimenggu Province, the Gaocheng Pb–Zn–Ag deposit in the Guangdong Province, and the Xinhua the deposit in Guangxi Province. At present, no granite intrusion has been found within a certain exploration depth in these deposits, which is the main reason for the controversy over the existence of their mineralization geological bodies. The discovery of intermediate-acidic dikes in the Qiandongshan–Dongtangzi mining area suggests that the hidden intrusions in the deeper parts of the mining area may be the metallogenic geological body. Meanwhile, the undiscovered hidden intrusions also contribute to the uncertainty surrounding the origin of the Qiandongshan–Dongtangzi lead–zinc deposit.

In summary, the formation of the Qiandongshan–Dongtangzi lead–zinc deposit is likely related to magmatic–hydrothermal activity. It is supported by the bulk of the evidence that magmatic activity not only provided the heat energy, but also supplied some ore-forming materials for lead–zinc mineralization. The Qiandongshan–Dongtangzi lead–zinc deposit is perhaps a stratabound magmatic hydrothermal lead–zinc deposit developed in the Late Triassic period of the Qinling orogenic belt. The mineralization mother rock is likely a concealed granite body, with the ore-forming structural plane in the contact surface between the limestone of the Gudaoling Formation and the phyllite of the Xinghongpu Formation. The ore-forming fluid is driven form magmatic–hydrothermal fluid, which constitutes a perfect mineralization system integrating ore-forming geological body, ore-forming structural plane, metallogenesis, and ore-forming fluid [18].

6.2. Prospecting Model

During the Indosinian period, the Qinling orogeny was triggered by the subduction collision of the Yangtze Craton, leading to extensive intermediate-felsic magmatic activity [16,66–68], At the same time, a large-scale compressional-shear deformation system was formed due to a series of WNW-oriented composite folds, brittle-ductile shear zones, faults and joints, as well as NEN- and NE-oriented faults and joints [42,69].

The extensive magmatic activity that occurred on a large scale not only served as a heat energy but also facilitated the mobilization of ore-forming elements (e.g., Pb and Zn) during their migration process. This, in turn, led to the release of ore-forming fluids and materials, resulting in the transport of significant amounts of zinc and lead-rich fluids. Driven by the temperature–pressure gradient and buoyancy effect [70], these fluids migrated towards the lower temperature and pressure regions along the WNW-trending fault structure that extended from the basement rock to the Devonian strata, and subsequently mixed with meteoric water infiltrating the Devonian strata and organic water present in the shallow part, thereby enhancing the mineralization process. As a result, a filling saddle-shaped main ore body was formed in the detachment space of the contact zone between the Gudaoling Formation limestone and the Xinghongpu Formation phyllite within the core of the anticline (Figure 12). Additionally, a small-scale vein-type lead–zinc ore body was formed as part of the ore-forming fluid, flowed through the axial faults and fissures present in the limestone. In the process of mineralization fluid, biolimestone and other rock formations have a

neutralization reaction with carbonate rocks due to their chemical activity, porous and permeable, or provide reducing agents and adsorption, the weakly acidic mineralizing fluid has a neutralization reaction with carbonate rocks, and carbonate rocks dissolve to promote sulfide precipitation, thereby facilitating mineralization [62]. It is worth noting that the lead–zinc mineralization observed in various locations and decompression–expansion sites within the ore cluster region can be attributed to mineralization occurring in different spatial structures during the same process [3,4,8,55].
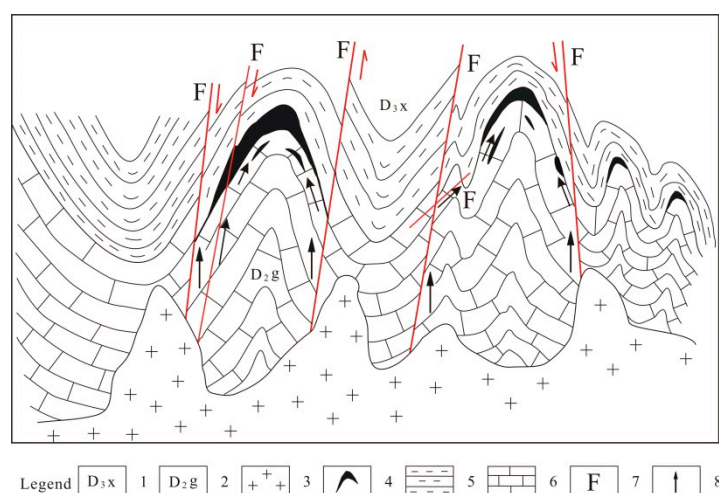
Figure 12. Metallogenic model of Qiandongshan–Dongtangzi Pb−Zn deposit. 1—Upper Devonian Xinghongpu Formation; 2—Middle Devonian Gudaoling Formation; 3—Triassic intermediate-acid rock mass; 4—Pb−Zn ore body; 5—Phyllite; 6—Limestone; 7—Faults; 8—Direction of magmatic hydrothermal fluid migration.

7. Ore-Controlling Factors and Prospecting Criteria

7.1. Ore-Controlling Factor

From the perspective of spatial occurrence characteristics of lead–zinc deposits, the ore-controlling factors of the lead–zinc deposits in the Fengtai orefield are basically the same, that is, they are controlled by the trinity "stratigraphy + stratigraphic position + structure".

The lead–zinc ore body in the Qiandongshan–Dongtangzi large lead–zinc deposit is located on the limestone side of the contact zone between the Middle Devonian Gudaoling Formation and the Upper Devonian Xinghongpu Formation, which is at the top of the Gudaoling Formation. This demonstrates that the occurrence of the lead–zinc ore body is controlled by stratigraphy.

The ore-hosted rock is dominated by silicified limestone, which is present in specific layers and macroscopically demonstrates the control of specific layers on lead–zinc deposits. This particular layer is the lithological interface (Si/Ca interface) and the carbonaceous rock layer [71,72] (Zhang, 2012; Shi et al., 2022). The interface between limestone and phyllite is the main ore-forming structural plane of lead–zinc ore body in Qiandongshan–Dongtangzi large lead–zinc deposits, serving as the transition boundary for physical and chemical conditions and a weak zone for tectonic activities. The occurrence of lead–zinc ore bodies often have high carbonaceous content. This is due to the occurrence of lithological interface sliding and thermal metamorphism during mineralization which leads to the precipitation of carbonaceous materials in the wall-rock, often resulting in the development of carbonaceous layers in the hanging wall of the ore body, forming a distinctive lithological layer.

The most obvious occurrence feature of lead–zinc ore bodies in the Fengtai orefield is that they are controlled by anticline structure. The Qiandongshan–Dongtangzi large lead–zinc deposit is controlled by the Qiandongshan–Dongtangzi complex anticline (level III) on the south side of the western end of the Qiandongshan–Shangtianba–Shuibaigou complex

anticline (level II). The secondary anticlines in the north branch anticline and the south branch anticline (level IV), respectively, control the No. I ore body and No. II ore body in the mining area. In addition, the fault structural plane controls the ore body, and the veined Pb-Zn ore body found along the inter-layer fracture zone within the limestone of Gudaoling Formation or the phyllite of the Xinghongpu Formation is the manifestation of structural ore control.

7.2. Prospecting Criterias

The contact interface between the limestone of the Middle Devonian Gudaoling Formation and the phyllite of the Upper Devonian Xinghongpu Formation is the stratigraphic marker for prospecting the Qiandongshan–Dongtangzi large Pb-Zn deposit. The anticlinal structures, especially the turning end and the wing of the secondary fold, serve as important structural indicators for mineral exploration. Silicified limestone is serves as an indicator for direct lithology exploration in the field. Silicification and dolomitization serve as the alteration indicators for mineral exploration. The development of lead–zinc mineralization mainly is often associated with low-resistance, high-polarization induced electrical anomalies, self-potential anomalies, and geochemical anomalies characterized by combinations of elements such as Pb, Zn, Au, Ag, As, and Sb. These anomalies serve as indirect indicators for mineral exploration from a physical and chemical perspective.

8. Prospecting Prediction and Verification

Based on the metallogenic model outlined above, the prospecting predictions primarily rely on the Si/Ca interface and the secondary anticline structure. A series of WNW-trending tight folds formed in the Fengtai orefield during the Indosinian period, which is the most favorable location for prospecting prediction. It is considered that the secondary anticlines (IV level) developed on both limbs of the Qiandongshan–Dongtangzi anticline (III level) favorable mineralization sites. Accordingly, we propose a novel prospecting verification strategy targeting the saddle of the secondary anticline in the Dongtangzi lead–zinc deposit section. Specifically, we have developed a prospecting verification scheme for the CZK8205 drill hole in the 82nd exploration line (Figure 13). It has been confirmed that a thick and extensive industrial ore body, containing Pb at a grade of 4.0% and Zn at a grade of 6.28%, with a true thickness of 5.35 m was discovered on the phyllite of the contact zone between bioclastic limestone and phyllite within the saddle of the secondary anticline. Subsequently, two additional drill holes, CZK8206 and CZK8207, were carried out on the south and north sides of the CZK8205 drill hole, respectively, in the two limbs of the secondary anticline. In the CZK8207 drill hole, a thick and rich industrial ore body with a Pb grade of 2.44%, a Zn grade of 6.82%, and a true thickness of 8.46 m was discovered. Exploration and mining activities have demonstrated that the known ore bodies exhibit a westward inclination with the Qiandongshan–Dongtangzi ore-controlling anticline. Moreover, the secondary anticline, which is similar to the primary ore-controlling anticline, is also inclined to the west and extends stably in a concealed mode. It is suggested that the extension of the ore body towards the west is highly probable, as supported by comprehensive research. To verify this hypothesis, two verification drill holes, CZK8604 and CZK8605, were conducted in the 86th line of the western extension of the ore body. The results of these drill holes revealed lead–zinc ore bodies with a Pb grade of 0.06%, a Zn grade of 6.59%, and a true thickness of 1.92 m for CZK8604, and a Pb grade of 0.89%, a Zn grade of 6.77%, and a true thickness of 2.64 m for CZK8605. Remarkably, the scale, thickness, and grade of this ore body is comparable to that of the II-1 main ore body.
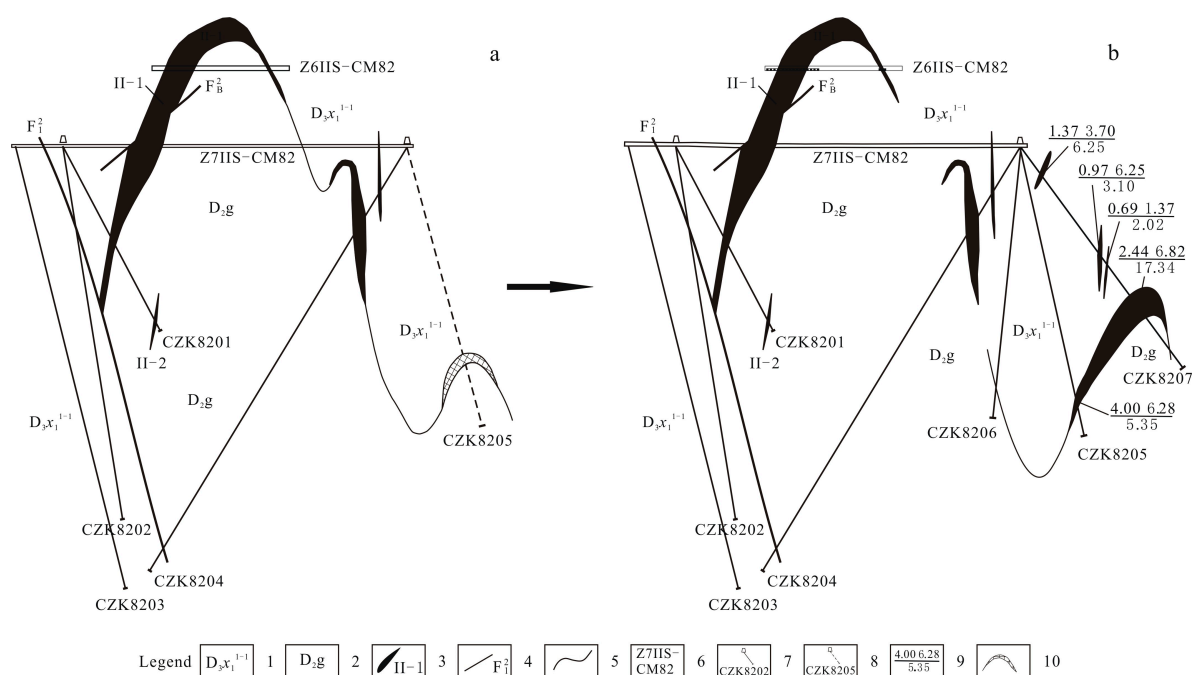
Figure 13. The Geological Profiles 82 Exploration Line of the Dongtangzi Lead–Zinc section. (**a**)—Prediction diagram; (**b**)—Verification diagram; 1—Calcareous phyllite intercalated with thin limestone in the first lithologic substratum of the first lithologic layer of the first lithologic member of the Xinghongpu Formation in the upper Devonian; 2—Thin–medium–thick bedded bioclastic microcrystalline limestone and crystalline limestone of the Gudaoling Formation in the Middle Devonian; 3—Lead–zinc deposit and number; 4—Faults and number; 5—Geological boundary; 6—Location and number of the tunnel; 7—Number of completed drilling; 8—Number of design drilling; 9—Lead grade(%) Zinc grade(%)/true thickness(m); 10—Prediction of ore body location approach of integrating a 'metallogenic model + prospecting prediction + drill hole verification' has proven to be a successful method for deep geological prospecting, which has accumulated successful experience for the discovery of a new lead–zinc deposit.

9. Conclusions

(1) The genesis of the Qiandongshan–Dongtangzi deposit should be probably attributed to a stratiform magmatic–hydrothermal origin. The deposit contains stratabound ore bodies in the anticlinal core, as well as vein-like and network-like ore bodies in the faults and fissures within the limestone. The ore bodies are controlled by the Si/Ca interface and the anticline structure.

(2) The Qiandongshan–Dongtangzi lead–zinc deposit formed in two stages. During the Indosinian period, a series of WNW-trending folds formed due to plate subduction and collision. This event also triggered large-scale intermediate-felsic magmatic activity that created structures for ore transportation and provided space for mineralization. In the late- to post-collision stage, magmatic fluids carrying ore-forming elements were deposited on the Si/Ca interface of the physical-chemical mutation. This interface formed in the contact zone between limestone of the Gudaoling Formation and phyllite of the Xinghongpu Formation at the core of an anticline.

(3) The detachment space created by the intersection of the anticline structure and the Si/Ca interface plays a critical role in metallogenic prediction. In particular, a series of WNW-trending secondary anticlines that have developed on the two limbs of the main ore-controlling anticline of the Qiandongshan–Dongtangzi large-scale lead–zinc deposit are the most favorable metallogenic sites and the preferred target for prospecting prediction. The drilling verification scheme was designed for the secondary anticline on the north limb of the main ore-controlling anticline in the Dongtangzi lead–zinc deposits based on this method.

(4)　The drilling verification of the secondary anticline located on the north limb of the Qiandongshan–Dongtangzi ore-controlling anticline has led to the discovery of a thick and rich industrial lead–zinc ore body. The success of this example sets a precedent for prospecting and prediction in the Qiandongshan–Dongtangzi mining area, and contributes to the accumulation of successful experience in deep exploration and blind prospecting within the Fengtai orefield.

References

1.　Qi, S.J.; Li, Y. *Lead-Zinc Metallogenic Belt of Devonian System in Qinling Mountains*; Geological Publishing House: Beijing, China, 1993.
2.　Jia, R.X.; Han, S.S.; Wei, H.M. Main Metallogenic Characteristics and Genetic Analysis of Gold Deposit in Fengtai Ore Field Qinling. *J. Xi'an Eng. Univ.* **1999**, *21*, 67–75. (In Chinese with English Abstract)
3.　Wang, R.T.; Wang, D.S.; Dai, J.Z. *Study on Synthetical Exploration Technology for Pb-Zn-Ag-Cur-Au Deposits in Major Mineralization Concentrated Region of Shannxi Area in Qinling Orogenic Belt*; Geological Publishing House: Beijing, China, 2012; pp. 1–262.
4.　Wang, R.T.; Zhang, G.L.; Li, Q.F.; Zhang, B.; Cheng, H.; Ji, Y.F. Metallogenic Regularity and Prospecting Prediction of Fengtai Pb-Zn-Au Ore Concentration Area in Qinling Mountains. *J. Earth Sci. Environ.* **2021**, *43*, 528–548. (In Chinese with English Abstract)
5.　Fang, W.X. Research on Mineral Geochemistry of Qiandongshan Large-sized Lead-zinc Deposit in Fengxian County, Shaanxi. *Acta Miner. Sin.* **1999**, *19*, 198–205. (In Chinese with English Abstract)
6.　Hu, Q.Q. The Mineralization Features, Mechanism and Metallogenic Regularity of the Fengtai Pb-Zn Polymetallic Ore Cluster in West Qinling, China. Ph.D. Thesis, Chinese Academy of Geological Sciences, Beijing, China, 2015.
7.　Zhang, Y.F.; Yang, T.; Yi, P.F.; Yao, Z.; He, Y.F. LA-ICP-MS Zircon Geochronology and Geochemistry of the Huahongshuping Granodiorite Pluton in South Qinling. *Geol. Explor.* **2018**, *54*, 300–314. (In Chinese with English Abstract)
8.　Wang, Y.T.; Hu, Q.Q.; Wang, R.T.; Gao, W.H.; Chen, S.C.; Wei, R.; Wang, C.A.; Wei, B.; Wei, S.W.; Tang, M.J. A New metallogenic model and its Significance in Search for Zn-Pb Deposits in Fengtai (Fengxian-Taibai) Polymetallic Ore Concentration Area, Shannxi Province. *Miner. Depos.* **2020**, *39*, 587–606. (In Chinese with English Abstract)
9.　Zhang, F. Magmatism and Mineralization of the Indosinian Period in the Fengtai Area, Qinling Mountains: Evidence of Geological Chronology and Geochemistry. Ph.D. Thesis, Peking University, Beijing, China, 2010.
10.　Wang, H.; Wang, J.P.; Liu, J.J.; Cao, R.R.; Hui, D.F.; Cheng, J.J. Mineralogy of the Xiba Granitoid Pluton in the Southern Qinling Orogenic Belt and Its Implications for Petrogenesis. *Geoscience* **2011**, *3*, 489–502. (In Chinese with English Abstract)
11.　Li, Q.F.; Wang, B.W.; Zhang, B. *A Summary of 1:50000 Jiingkou (I48E013012), Jiangkou (I48E014021) and Guanshan (I48E012021), Mineral Geological Survey for Shaanxi*; Baoji 717 Corps Limited of Norhwest Nonferrous Geological and Mining Group: Baoji, China, 2019. (In Chinese)
12.　Wang, J.L.; He, B.C.; Li, J.Z. *Qinling Type Lead and Zinc Mineral Deposits in China*; Geological Publishing House: Beijing, China, 1996; pp. 1–264. (In Chinese)
13.　Zhang, F.X.; Du, X.H.; Wang, W.T.; Qi, Y.L. Mineralization responsed to mesozoic geological evolution of the Qinling orogen and its environs. *Chin. J. Geol.* **2004**, *39*, 486–495. (In Chinese with English Abstract)
14.　Wang, R.T. Study on Metallogenic Model for Typic Meta1 Ore Deposits and Exploration Predicting of Qinling Orogenic Belt in Shannxi Province, China. Ph.D. Thesis, University of Geosciences, Beijing, China, 2005; pp. 1–158.
15.　Feng, J.Z.; Wang, D.B.; Wang, X.M.; Shao, S.C. Stable Isotope Geochemistry of Three Typical Gold Deposits in the West Qinling. *Geol. China* **2004**, *31*, 78–84. (In Chinese with English Abstract)
16.　Chen, S.C.; Wang, Y.T.; Yu, J.J.; Hu, Q.Q.; Zhang, J.; Wang, R.T.; Gao, W.H.; Wang, C.A. Petrogenesis of Triassic granitoids in the Fengxian–Taibai ore cluster, Western Qinling Orogen, central China: Implications for tectonic evolution and polymetallic mineralization. *Ore Geol. Rev.* **2020**, *123*, 103577. [CrossRef]

17. Zhang, G.L.; Wang, R.T.; Tian, T.; Ding, K.; Gao, W.H.; Guo, Y.Y. Geological-geochemical Characteristics and Genesis of Dongtangzi Pb-Zn Deposit in Fengxian-Taibai Ore Concentration Area of Shaanxi, China. *J. Earth Sci. Environ.* **2018**, *40*, 520–534. (In Chinese with English Abstract)

18. Ye, T.Z.; Lu, Z.C.; Pang, Z.S. *Theory and Method of Prospecting Prediction in Exploration Area (Pandect)*; Geological Publishing House: Beijing, China, 2015. (In Chinese with English Abstract)

19. Li, Y.Q.; Wang, R.T.; Meng, D.M.; Dai, J.Z.; Huang, C.Q. Geological Characteristics and Prospecting Direction of Taishanmiao Copper Deposits in Fengxian County, Shaanxi Province. *Northwest. Geol.* **2015**, *48*, 169–175. (In Chinese with English Abstract)

20. Huang, Z.Y.; Lu, R.N. Zoning Characteristics and Index of Primary Geochemical Anomalies in Qiandongshan Pb-Zn Deposit, ShanXi Province, China. *Geol. Prospect.* **2003**, *3*, 39–44. (In Chinese with English Abstract)

21. Long, H.S.; Luo, T.Y.; Huang, Z.L.; Zhou, M.Z.; Yang, Y.; Qian, Z.K. Rare Earth Element and Trace Element Geochemistry of Pyrite Ores in the Laochang Large Size Silver Ploymetallic Deposit of Lancang, Yunnan Province, China. *Acta Miner. Sin.* **2011**, *31*, 462–473. (In Chinese with English Abstract)

22. Yan, Q.J.; Wei, X.Y.; Ye, M.F.; Zhou, H.B.; Zhou, N.C. Determination of Composition of Pyrite in the Baishantang Copper Deposit by Laser Ablation-inductively Coupled Plasma-mass Spectrometry and Electron Microprobe. *Rock Miner. Anal.* **2016**, *35*, 658–666. (In Chinese with English Abstract)

23. Zeng, Y.C.; Huang, S.J.; Jia, G.X.; Chen, Y.R. Eigenelements of Some Metallic Minerals in the Magmatic Hydrothermal and Stratabound Pb-Zn Deposits and Their Geological Significance. *Geol. Prospeting* **1985**, *21*, 28–33. (In Chinese)

24. Han, Z.X. The Typomorphic Characteristic of the Sphalerite in the Qinling Devonian System Lead-zinc Metallogenic Belt. *J. Xi'an Coll. Geol.* **1994**, *16*, 12–17. (In Chinese with English Abstract)

25. Wang, R.T.; Li, F.L.; Chen, E.H.; Dai, J.Z.; Wang, C.A.; Xu, X.F. Geochemical Characteristics and Prospecting Prediction of the Bafangshan-Erlihe Large Lead-zinc Ore Deposit, Feng County, Shaanxi Province, China. *Acta Petrol. Sin.* **2011**, *27*, 779–793. (In Chinese with English Abstract)

26. Li, T. Application of the elemental abundance. *Geol. Explor.* **1981**, *6*, 1–6. (In Chinese)

27. Wang, L.; Tian, T.; Li, W.; Zhang, B.; Zhang, G.L.; Wang, F.; Zheng, S.X. Discussion on the geochemistry and evolution of Xiba rock mass in the central part of Fengtai high ore concentration area. *Gold* **2021**, *42*, 25–30. (In Chinese with English Abstract)

28. Zhang, G.L.; Wang, L.; Tian, T. *Achievement Report of Sub-Project of Prospecting and Prediction in Fengtai Ore Gathering Area of Shaanxi Province*; Baoji 717 Corps Limited of the Northwest Nonferrous Geological and Mining Group: Baoji, China, 2019.

29. Han, F.; Sun, H.T. Metallogenic system of sedex type deposits: A review. *Earth Sci. Front.* **1999**, *6*, 139–157. (In Chinese)

30. Leach, D.L.; Sangster, D.F.; Kelley, K.D.; Large, R.R.; Garven, G.; Allen, C.R.; Gutzmer, J.; Wahers, S. Sediment-hosted lead-zinc deposits: A global perspective. *Econamic Geol.* **2005**, *100*, 561–607.

31. Li, H.Z.; Zhou, Y.Z.; Yang, Z.J.; Gu, Z.H.; Lv, W.C.; He, J.G.; Li, W.; An, Y.F. Geochemical Characteristics and Their Geological Implications of Cherts from Bafangshan-Erlihe Area in Western Qinling Orogen. *Acta Petrol. Sin.* **2009**, *25*, 3094–3102. (In Chinese with English Abstract)

32. Ohmoto, H. Stable Isotope Geochemistry of Ore Deposits. *Rev. Miner. Geochem.* **1986**, *16*, 491–559.

33. Liu, B.Z.; Wang, J.P.; Zeng, X.T.; Wang, K.X.; Cao, R.R.; Cheng, J.J. Ore fluid and geochemical characteristics of Yanfangwan Pb-Zn deposit in Shaanxi Province. *Contrib. Geol. Miner. Resour. Res.* **2013**, *28*, 50–57. (In Chinese with English Abstract)

34. Wang, X.; Tang, R.Y.; Li, S.; Li, Y.X.; Yang, M.J.; Wang, D.S.; Guo, J.; Liu, P.; Liu, R.D.; Li, W.Q. *Oro-Geny and Metal Mineralization of Qinling Area*; Metallurgical Industry Press: Beijing, China, 1996. (In Chinese)

35. Jiang, X.M. A Discussion on the Genesis and Oreforming Mechanism of the Hogeqi Cu-Pb-Zn Deposit. *J. Miner. Deposits* **1983**, *4*, 1–10. (In Chinese with English Abstract)

36. Fu, C.; Wang, J.P.; Peng, R.M.; Liu, J.J.; Liu, Z.J.; Liu, Z.M. Features of Sulfur Isotope of the Jiashengpan Lead-Zinc-Sulfur Dposit in Inner Mongolia and Its Genesis Significance. *J. Geosci.* **2010**, *24*, 34–41. (In Chinese with English abstract)

37. Zhang, M.C.; Chen, R.Y.; Ye, T.Z.; Li, J.C.; Lü, Z.C.; He, X.; Chen, H.; Yao, L. Genetic study on the Qixiashan Pb-Zn polymetallic deposit in Jiangsu Province: Evidence from fluid inclusions and H-O-S-Pb isotopes. *J. Acta Petrol. Sin.* **2017**, *33*, 3453–3470. (In Chinese with English Abstract)

38. Liu, T.T.; He, Z.W.; Cui, X.L.; Ni, Z.Y.; Liu, H.F.; Zhang, J.S. Model Construction and Prospecting Prediction of Lead-Zinc Polymetallic Ore Deposits Based on GIS Information Method. *J. Guilin Univ. Technol.* **2011**, *4*, 511–515. (In Chinese with English Abstract)

39. Ren, P.; Liang, T.; Liu, K.L.; Liu, L.; Lu, L.; Zhang, W.J. Geochemistry of Sulfur and Lead Isotopic Compositions of Sedex Lead-zincDeposits in Fengtai Mineral Cluster Region of Qinling Mountains. *J. Northwestern Geol.* **2014**, *47*, 137–149. (In Chinese with English Abstract)

40. Wei, H.M.; Zhang, Z.F. Lithofacies during the ore-forming period and their prospecting significance in the Qiandongshan-Tanjiagou area of the Fengtai lead-zinc ore field. *Northwest Geol.* **1987**, *5*, 6–11. (In Chinese)

41. Zhang, F.X.; Wang, J.F. Devoninasyngenetic faults and lith of acies in relation to submarine exhalative sedimentary lead- zinc deposits in Qinling area, Shaanxi Province. *J. Miner. Deposits* **1991**, *3*, 217–231. (In Chinese with English Abstract)

42. Zhang, H.F.; Ouyang, J.P.; Lin, W.L.; Chen, Y.L. Pb, Sr, Nd, Isotope Composition of Ningshan Granitoids, South Qinling and their Deep Geological Information. *Acta Petrrologica Miner.* **1997**, *16*, 22–31. (In Chinese with English Abstract)

43. Wang, R.T.; Wang, T.; Gao, Z.J.; Chen, E.H.; Liu, L.X. The Main Metal Deposits Metallogenic Series and Exploration Direction in Feng-Tai Ore Cluster Region, Shaanxi Province. *Northwest Geol.* **2007**, *40*, 77–84. (In Chinese with English Abstract)

44. Wang, D.S.; Wang, R.T.; Dai, J.Z.; Wang, C.A.; Li, J.H.; Chen, L.X. "Dual Ore controlling Factors" Characteristics of Metallic Deposits in the Qinling Orogenic Belt. *Acta Geol. Sin.* **2009**, *83*, 1719–1729. (In Chinese with English Abstract)

45. Zhang, F.; Liu, S.W.; Li, Q.G.; Sun, Y.L.; Wang, Z.Q.; Yan, Q.R.; Yan, Z. Re-Os and U-Pb Geochronology of the Erlihe Pb-Zn Deposit Qinling Orogenic Belt, Central China and Constraints on Its Deposit Genesis. *Acta Geol. Sin. (Engl. Ed.)* **2011**, *85*, 673–682. [CrossRef]

46. Hu, Q.Q.; Wang, Y.T.; Wang, R.T.; Li, J.H.; Dai, J.Z.; Wang, S.Y. Ore-forming time of the Erlihe Pb-Zn deposit in the Fengxian-Taibai ore concentration area, Shaanxi Province: Evidence from the Rb-Sr isotopic dating of sphalerites. *Acta Petrol. Sin.* **2012**, *28*, 258–266. (In Chinese with English Abstract)

47. Zhang, F.; Liu, S.W.; Li, Q.G.; Wang, Z.Q.; Han, Y.G.; Yang, K.; Wu, F.H. LA-ICP-MS Zircon U-Pb Geochronology and Geological Significance of Xiba Granitoids from Qinling, Central China. *Acta Sci. Nat. Univ. Pekin.* **2009**, *45*, 833–840. (In Chinese with English Abstract)

48. Hu, Q.Q.; Wang, Y.T.; Mao, J.W.; Liu, S.W. Timing of the Formation of the Changba-Lijiagou Pb-Zn Ore Deposit, Gansu Province, China: Evidence from Rb-Sr Isotopic Dating of Sulfides. *J. Asian Earth Sci.* **2015**, *103*, 350–359. [CrossRef]

49. Wang, H. The Features of Magmatic Rocks in Shangwang Gold Mine, Shanxi Province and Its Implication on Gold Mineralization. Ph.D. Thesis, China University of Geosciences, Beijing, China, 2012.

50. Yang, P.T.; Liu, S.W.; Li, Q.G.; Wang, Z.Q.; Zhang, F.; Wang, W. Chronology and Petrogenesis of the Hejiazhuang Granitoid Pluton and Its Constraints on the Early Triassic Tectonic Evolution of the South Qinling Belt. *Sci. China Earth Sciences* **2013**, *43*, 1874–1892. (In Chinese) [CrossRef]

51. Liu, S.W.; Yang, P.T.; Li, Q.G.; Wang, Z.Q.; Zhang, W.Y.; Wang, W. Indosinian Granitoids and Orogenic Processes in the Middle Segment of the Qinling Orogen, China. *J. Jilin Univ. (Earth Sci. Ed.)* **2011**, *41*, 1928–1943. (In Chinese with English Abstract)

52. Zhang, Z.Q.; Zhang, G.W.; Liu, D.Y. *Isotopic Geochronology and Geochemistry of Ophiolites, Granites and Clastisedimentary Rocks in the Qinling-Dabie Orogenic Belt*; Geological Publishing House: Beijing, China, 2006.

53. Lü, X.Q.; Wang, X.X.; Ke, C.H.; Li, J.B.; Yang, Y.; Meng, X.Y.; Nie, Z.R.; Zhang, P.F. LA-ICP-MS zircon U-Pb dating of Taibai pluton in North Qinling Mountainsand its geological significance. *Miner. Depos.* **2014**, *33*, 37–52. (In Chinese with English Abstract)

54. Meng, X.Y.; Wang, X.X.; Ke, C.H.; Li, J.B.; Yang, Y.; Lü, X.Q. LA-ICP-MS zircon U-Pb age, geochemistry and Hf isotope of the granitoids from Huayang pluton in South Qinlig orogen: Constraints on the genesis of Wulong plutons. *Geol. Bull. China* **2013**, *32*, 1704–1719. (In Chinese with English Abstract)

55. Wang, Y.T.; Mao, J.W.; Hu, Q.Q.; Wei, R.; Chen, S.C. Characteristics and Metallogeny of Triassic Polymetallic Mineralization in Xicheng and Fengtai Ore Cluster Zones, West Qinling, China and Their Implications for Prospecting Targets. *J. Earth Sci. Environ.* **2021**, *43*, 409–435. (In Chinese with English Abstract)

56. Wang, J.H.; Zhang, F.X.; Yu, Z.P.; Yu, L. Minerogenetic series of metallic ore deposits in the Qinling Mountains and tectonodynamic background of the continental orogenic belts. *Geol. China* **2002**, *29*, 192–196. (In Chinese with English Abstract)

57. Lu, X.X.; Li, M.L.; Wang, W.; Yu, Z.P.; Shi, Y.Z. Indosinian movement and metallogenesis in Qinling orogenic belt. *Miner. Depos.* **2008**, *27*, 762–773. (In Chinese with English Abstract)

58. Chen, Y.J. Indosinian tectonic setting, magmatism and metallogenesis in Qinling Orogen, central China. *Geol. China* **2010**, *37*, 854–865. (In Chinese with English Abstract)

59. Shi, K.; Du, J.G.; Wan, Q.; Chen, F.; Cai, Y.; Cao, J.Y.; Wu, L.B.; Wang, L.M.; Tan, D.X. Chronology study of the Mesozoic intrusive rocks in the Tongling ore-cluster region, Anhui, and its metallogenic significance. *Acta Geol. Sin.* **2019**, *93*, 1096–1112. (In Chinese with English Abstract)

60. Hennet, R.J.C.; Crerar, D.A.; Schwartz, J. Organic complexes in hydrothermal systems. *Econ. Geol.* **1988**, *83*, 742–764. [CrossRef]

61. Giordano, T.H.; Barnes, H.L. Lead transport in Mississippi Valley-type ore solutions. *Economic Geol.* **1981**, *76*, 2200–2211. [CrossRef]

62. Barmes, H.L.; Gould, W.W. Hydrothermal replacement of carbonates by sulfdes. In Proceedings of the 7th International Symposium on Water-Rock Interaction, Park City, UT, USA, 13–18 July 1992; pp. 1565–1567.

63. Lu, J.C.; Yuan, Z.Q. Experimental Studies of Organic—An Complexes and their Stability. *Geochimica* **1986**, *1*, 66–77. (In Chinese)

64. Seward, T.M.; Barnes, H.L. Metal transport by hydrothermal ore fluids. In *Geochemistry of Hydrothermal Ore Deposits*; Barnes, H.L., Ed.; John Wiley & Sons, Inc.: New York, NY, USA, 1997.

65. Tagirov, B.R.; Seward, T.M. Hydrosulfide/sulfide complexes of zine to 250 °C and the thermodynamic properties of sphalerite. *Chem. Geol.* **2010**, *269*, 301–311. [CrossRef]

66. Deng, Z.B.; Liu, S.W.; Zhang, W.Y.; Hua, F.Y.; Li, Q.G. Petrogenesis of the Guangtoushan granitoid suite, central China: Implications for Early Mesozoic geodynamic evolution of the Qinling Orogenic Belt. *Gondwana Res.* **2016**, *30*, 112–131. [CrossRef]

67. Hu, F.Y.; Liu, S.W.; Zhang, W.Y.; Deng, Z.B.; Chen, X.A. Westward propagating slab tear model for Late Triassic Qinling Orogenic Belt geodynamic evolution: Insights from the petrogenesis of the Caoping and Shahewan intrusions, central China. *Lithos* **2016**, *262*, 486–506. [CrossRef]

68. Xiong, X.; Zhu, L.M.; Zhang, G.W.; Santosh, M.; Jiang, H.; Zheng, J.; Guo, A.L.; Ding, L.L. Petrogenesis and tectonic implications of Indosinian granitoids from Western Qinling Orogen, China:Products of magma-mixing and fractionation. *Geosci. Front.* **2020**, *11*, 1305–1321. [CrossRef]

69. Wang, Y.T.; Chen, S.C.; Hu, Q.Q.; Zhang, J.; Liu, X.L.; Huang, S.K. Tectonic controls on polymetallic mineralization in the Fengxian-Taibai ore cluster zone, western Qinling, Shannxi Province. *Acta Petrol. Sin.* **2018**, *34*, 1959–1976. (In Chinese with English Abstract)

70. Cox, S.F. Structural and isotopic constraints on fluid flow regimes and fluid pathways during upper crustal deformation: An example from the Taemas area of the Lachlan Orogen, SE Australia. *J. Geophys. Res.* **2007**, *112*, B08208. [CrossRef]
71. Zhang, C.Q.; Ye, T.Z.; Wu, Y.; Wang, C.H.; Ji, H.; Li, L.; Zhang, T.T. Discussion on controlling role of Si-Ca boundary in locating Pb-Zn deposits and its prospecting significance. *Miner. Depos.* **2012**, *31*, 405–416. (In Chinese with English Abstract)
72. Shi, Y.H.; Wang, Y.; Chen, B.L.; Tan, R.W.; Gao, Y.; Shen, J.H. Characteristics of silicon-calcium surface ore-controlling in Fengtai ore-concentration areas, West Qinling Mountains: Examples from Qiandongshan Pb-Zn deposit. *Geol. China* **2022**, *49*, 226–240. (In Chinese with English Abstract)